AD-A035 506

SCATHA SATELLITE INSTRUMENTATION REPORT

THERMAL PLASMA ANALYZER; RAPID SCAN PARTICLE

DETECTOR; ELECTRON BEAM SYSTEM; POSITIVE

ION BEAM SYSTEM

AIR FORCE GEOPHYSICS LABORATORY

HANSCOM AIR FORCE BASE, MASSACHUSETTS

10 SEPTEMBER 1976

AFGL-TR-76-0207
AIR FORCE SURVEYS IN GEOPHYSICS, NO. 352

SCATHA Satellite Instrumentation Report:

Thermal Plasma Analyzer
Rapid Scan Particle Detector
Electron Beam System
Positive Ion Beam System

ARTHUR L PAVEL, Capt, USAF (Editor)

10 September 1976

DDC

FEB 11 1977

A

SPACE PHYSICS DIVISION   PROJECT ILIR

AIR FORCE GEOPHYSICS LABORATORY

HANSCOM AFB, MASSACHUSETTS 01731

AIR FORCE SYSTEMS COMMAND, USAF

ADA035506

REPORT DOCUMENTATION PAGE		READ INSTRUCTIONS BEFORE COMPLETING FORM
1. REPORT NUMBER AFGL-TR-76-0207	2. GOVT ACCESSION NO.	3. RECIPIENT'S CATALOG NUMBER
4. TITLE (and Subtitle) **SCATHA SATELLITE INSTRUMENTATION REPORT:** **THERMAL PLASMA ANALYZER; RAPID SCAN PARTICLE** **DETECTOR; ELECTRON BEAM SYSTEM; POSITIVE ION** **BEAM SYSTEM**		5. TYPE OF REPORT & PERIOD COVERED Scientific. Final
		6. PERFORMING ORG. REPORT NUMBER AFSG, No. 352
7. AUTHOR(s) Arthur L. Pavel, Capt, USAF (Editor)		8. CONTRACT OR GRANT NUMBER(s)
9. PERFORMING ORGANIZATION NAME AND ADDRESS Air Force Geophysics Laboratory (PHG) Hanscom AFB, Massachusetts 01731		10. PROGRAM ELEMENT, PROJECT, TASK AREA & WORK UNIT NUMBERS 61102F ILIR4E01
11. CONTROLLING OFFICE NAME AND ADDRESS Air Force Geophysics Laboratory (PHG) Hanscom AFB, Massachusetts 01731		12. REPORT DATE 10 September 1976
		13. NUMBER OF PAGES 56
14. MONITORING AGENCY NAME & ADDRESS(if different from Controlling Office)		15. SECURITY CLASS. (of this report) Unclassified
		15a. DECLASSIFICATION/DOWNGRADING SCHEDULE

16. DISTRIBUTION STATEMENT (of this Report)

Approved for public release; distribution unlimited.

17. DISTRIBUTION STATEMENT (of the abstract entered in Block 20, if different from Report)

18. SUPPLEMENTARY NOTES
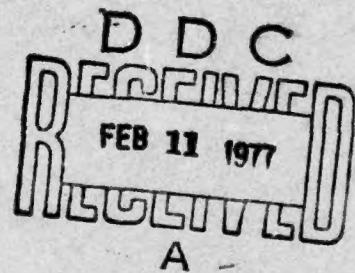
This research was supported by the Air Force In-house Laboratory Independence Research Fund.

19. KEY WORDS (Continue on reverse side if necessary and identify by block number)

Satellite instrumentation
Spacecraft survivability
Synchronous orbit
Satellite design

20. ABSTRACT (Continue on reverse side if necessary and identify by block number)

The Air Force Geophysics Laboratory will furnish four experiments for the synchronous research satellite SCATHA (Spacecraft Charging at High Altitudes) scheduled for launch in 1978. These instruments include: (1) Boom and surface mounted gridded probes to measure the thermal (0 to 100 eV) plasma environment and the structure of the satellite photo-sheath; (2) A combination of electrostatic analyzers and solid state spectrometers to measure the plasma

DD FORM 1 JAN 73 **1473** EDITION OF 1 NOV 65 IS OBSOLETE

Unclassified

20.   (Cont)

particle fluxes (50 eV to 10 MeV) responsible for the spacecraft charging
phenomena and transient charging efects; (3) An electron beam system able
to eject electrons with from 50 eV to 3 keV in energy to attempt to correct for
charging caused by environmental electrons; (4) An ion beam system able to
eject ionized xenon with 1 keV and 2.5 keV energies, to attempt to duplicate
charging caused by environmental electrons.   These instruments will be part
of the total SCATHA instrumentation which consists of engineering and envir-
onmental definition experiments.   Acting in concert, these instruments will
test charge neutralizing procedures and provide data to specify design criteria
for future synchronous satellites.

This technical report has been reviewed and
is approved for publication.

FOR THE COMMANDER:
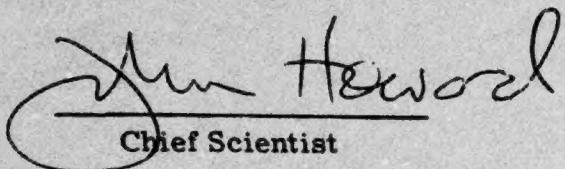
Chief Scientist

Qualified requestors may obtain additional copies from the
Defense Documentation Center. All other shoud apply to the
National Technical Information Service.

1(a)

Contents

Illustrations

3

4

Tables

5

SCATHA Satellite Instrumentation Report:

Thermal Plasma Analyzer;
Rapid Scan Particle Detector;
Electron Beam System;
Positive Ion Beam System

1. Introduction

1-1. INTRODUCTION

In this report the details of the design of four instruments which have been developed by the Air Force Geophysics Laboratory are given. These instruments will be launched into synchronous orbit aboard the research satellite SCATHA (Spacecraft Charging At High Altitudes).[1] They are now in various stages of fabrication. Launch of the SCATHA satellite by a Delta booster is scheduled for mid-1978. The Martin-Marietta Corporation has been chosen as the satellite contractor. Figure 1-1 shows the Martin-Marietta design for the SCATHA satellite.

It was found that, in the presence of a magnetospheric substorm, synchronous satellites could charge to high negative potentials. Potentials of several kilovolts for those periods in which the satellite was eclipsed by the earth's shadow were not uncommon. Even while the satellite was sunlit and emitting photoelectrons that could mediate the charge buildup, potentials of several hundred volts were measured.

The buildup of charge aboard synchronous satellites was subsequently linked to the anomalous behavior of several DOD and commercial satellites.[2] In response to these still not fully understood events, a research program including the research satellite SCATHA was developed. The entire program, which is still being

1. DeForest, S.E. (1972) Spacecraft charging, J. Geo. Res. 77:651-658.

2. McPherson, D.A., Cauffman, D.P., and Schober, W. (1975) Spacecraft Charging at High Altitudes — The SCATHA Satellite Program, AIAA Paper 75-19.

Preceding page blank
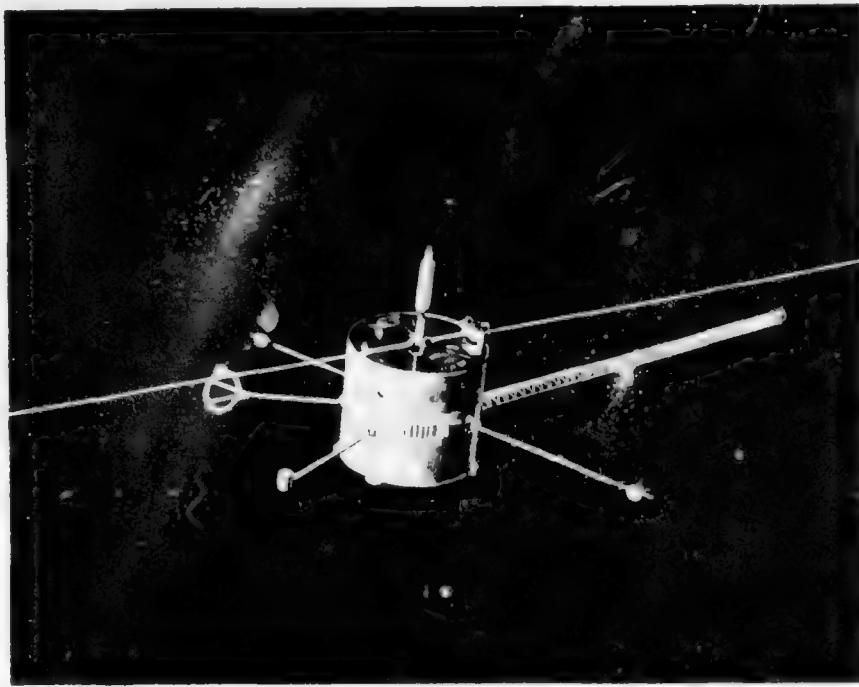
Figure 1-1.   Martin-Marietta Design Concept for the SCATHA Satellite

formulated, includes space measurements from the SCATHA satellite, laboratory
measurements, and theoretical calculations and charge buildup modeling studies.
The Air Force Geophysics Laboratory is an active participant in several aspects of
these spacecraft charging studies.   The data provided by the SCATHA satellite will
become part of laboratory and theoretical studies and form a basis for understand-
ing and correcting for the buildup of charge on a synchronous satellite.

1-2.   SCATHA SATELLITE

The SCATHA satellite orbit will be elliptical with an apogee at 22764 nmi and a
perigee at 15882 nmi above sea level.   These distances conform to from 5.6 earth
radii to 7.6 earth radii, and bracket the region of primary interest, which is a
synchronous orbit at 6.6 earth radii.   The orbit is nominally inclined between 0 and
2.5 deg with respect to the earth's equatorial plane.   The orbit will drift in the
equatorial plane at the rate of a few degrees per day.   The satellite spin rate will
be near one revolution per minute, with the spin axis in the orbital plane and per-
pendicular to the earth-sun line.

8

The total complement of SCATHA instrumentation will include 12 separate sets of experiments. These include several engineering experiments to measure surface potentials and the electrical effects of spacecraft charging on satellite surface and subsystems. There are also several experiments designed to measure the characteristic environmental fields and particle fluxes. Two of the Air Force Geophysics Laboratory experiments fall into this group, the Thermal Plasma Analyzer and Rapid Scan Particle Detector. The Air Force Geophysics Laboratory is also providing an electron beam system and a positive beam system for the active study of spacecraft charging. The engineering, environmental, and active control experiments have been selected so as to work in concert and relate cause and effect on spacecraft charging.

Contents

2. Thermal Plasma Analyzer

W. Sullivan, M. Smiddy, R. Sagalyn
Air Force Geophysics Laboratory
Hanscom AFB, Massachusetts
P. Anderson
Regis College
Weston, Massachusetts

2-1. INTRODUCTION

The Thermal Plasma Analyzer consists of three gridded sensors. Two sensors are mounted on a boom 3 meters from the nearest space vehicle body-mounted components. The third sensor is body mounted on the conducting end of the space vehicle. The normal to the aperture of one boom sensor is parallel to the normal to the aperture of the surface sensor. They are also parallel to the space vehicle spin momentum vector. The second boom sensor is perpendicular to the spin vector. The experiment will measure, by retarding potential analysis, the environmental electron and ion densities in the range 10^{-1} to 10^4 per cm^3 and particle energies in the range 0. 1 to 100 eV. Figure 2-1 shows the type of gridded sensor used to make thermal plasma measurements.

The Thermal Plasma Analyzer will measure the direction and magnitude of the plasma bulk motion, the density and temperature of the plasma 'bath' in which the satellite is immersed, and investigate spacecraft-plasma interaction mechanisms by measuring fluctuation in vehicle potential and charging and discharge currents to

11 **Preceding page blank**

Figure 2-1. Gridded Sensor Similar to the Three Sensors Used on the
SCATHA Thermal Plasma Analyzer

the satellite due to environmental factors such as solar illumination, satellite
motion, plasma temperature, density, and motion variations during quiet and dis-
turbed conditions. It is also aimed at studies of these properties under controlled
conditions when the spacecraft potential is varied by means of an electron gun.
These constitute some of the prime measurements required to understand and solve
the problem of spacecraft charging at high altitudes.

Basic mechanical design of the gridded probe is shown in Figure 2-2. The com-
bined measurements from the surface mounted sensor and the boom mounted units
make it possible to ascertain the influence of photoelectrons from the spacecraft
surface. Photoelectron production within the sensor is further minimized by restrict-
ing the sensor aperture field of view to a 15° half-angle cone. Depending on the volt-
age of the collector and stepped grid, the electrons or positive ions will be measured.

12
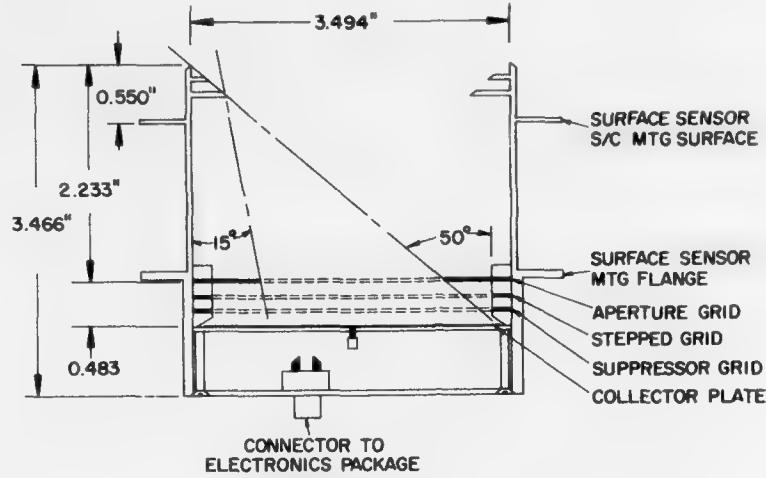
Figure 2-2. Surface and Boom Mounted Instruments

During disturbed conditions the vehicle potential may exceed 100V negative. In this case the potential is determined from the positive ion sensor where the thermal ions arrive at the vehicle with average energies equal to their thermal energy plus that imparted by the energy equivalent of the spacecraft potential.

The electrical configuration of the sensors is shown in Figure 2-3. Using ground commands A, B, and C, the boom and surface mounted sensors can be operated in a large number of ion or electron modes. Commands D, E, F, and G select eight (8) aperture-bias levels ranging from -50V to +50V.

The surface mounted sensor is shown in Figure 2-4 and the boom mounted sensors are shown in Figure 2-5. Figure 2-6 is a drawing of the electronics package, which will contain the electronics for the three sensor heads.

2-2. PAYLOAD CIRCUIT DESCRIPTIONS

The system Block Diagram (Figure 2-7) shows the major experiment components in addition to specific circuits within the main electronics package SC6-3.

The following paragraphs provide a brief description of these circuits and their relation to one another.

13
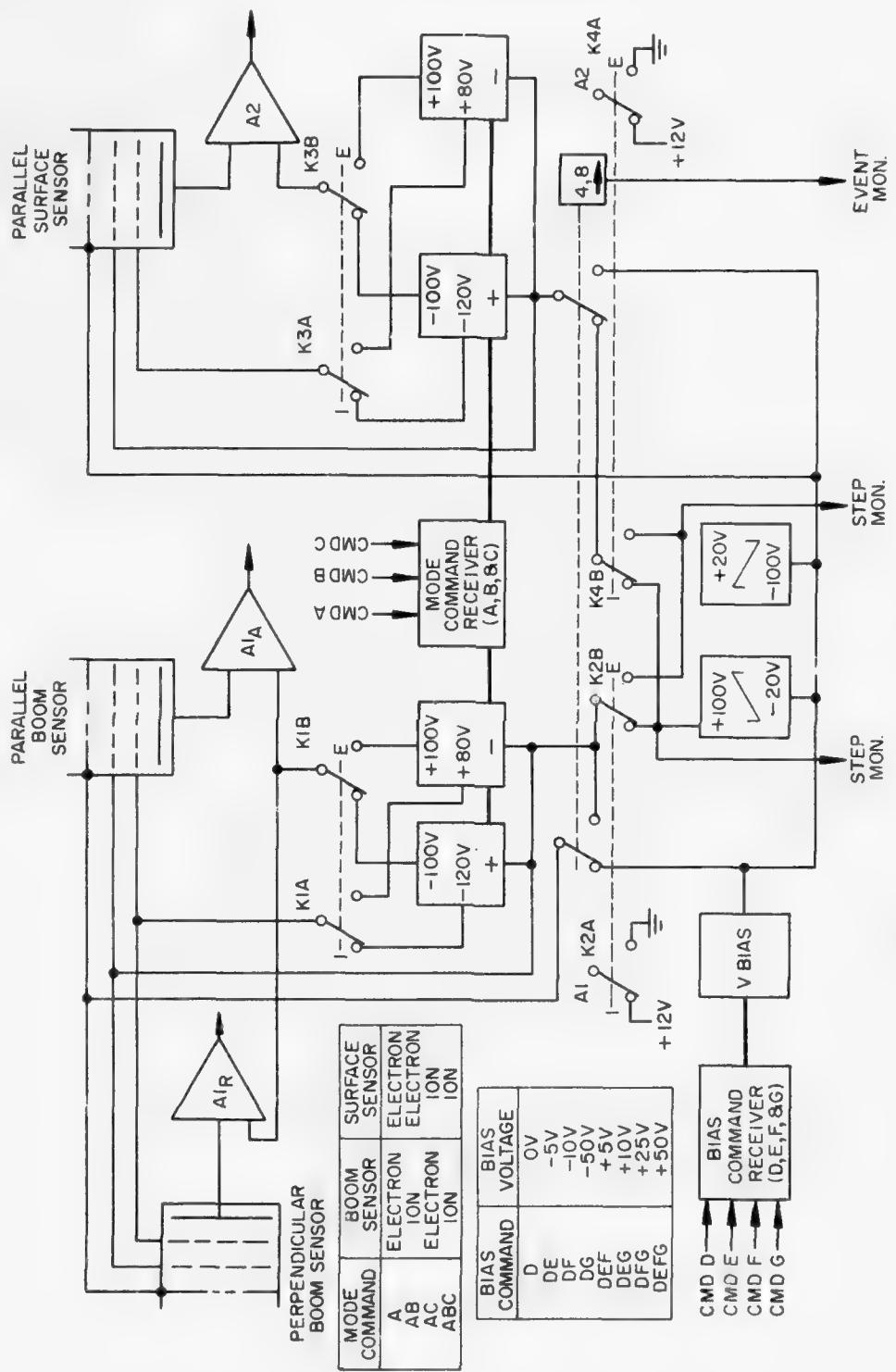
Figure 2-3. Sensor Electrical Configuration

14

SENSOR MOUNTING
FLANGE

S/C SURFACE
MOUNTING FLANGE

3.464"

Figure 2-4. Surface
Sensor

0.550"

2.233"

3.466"

WEIGHT = 1.0 lb
(ESTIMATED)

6.875"

PERPENDICULAR
BOOM SENSOR

3.564"

5.500"

BOOM

PARALLEL
BOOM SENSOR
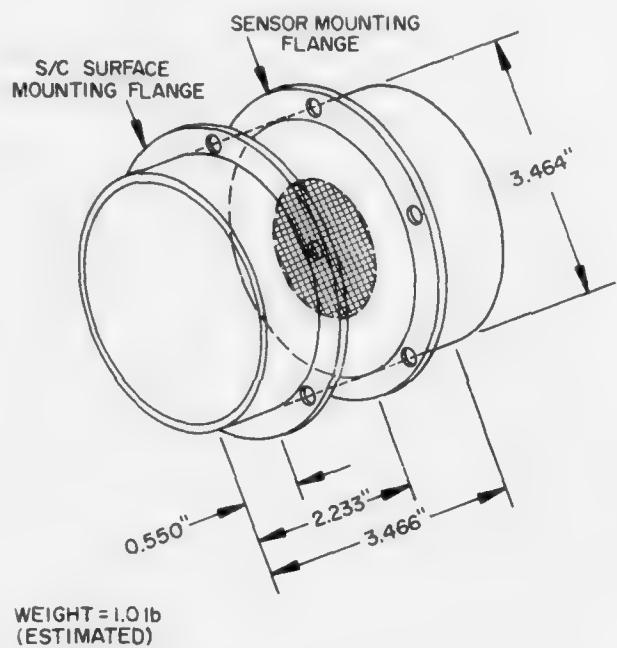
WEIGHT 1.8 lb (ESTIMATED)
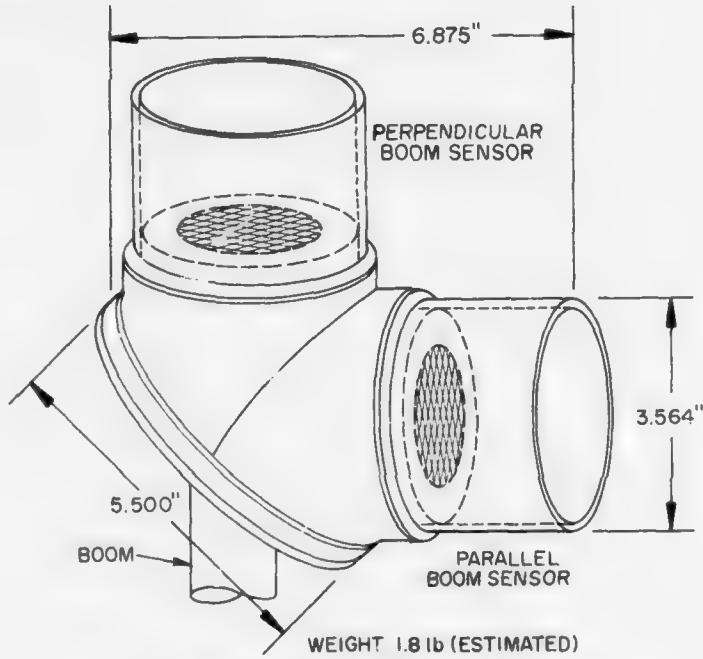
Figure 2-5. Boom Mounted Sensors

15

WEIGHT 4 lb (estimated)

6.0 in

6.0 in

6.0 in
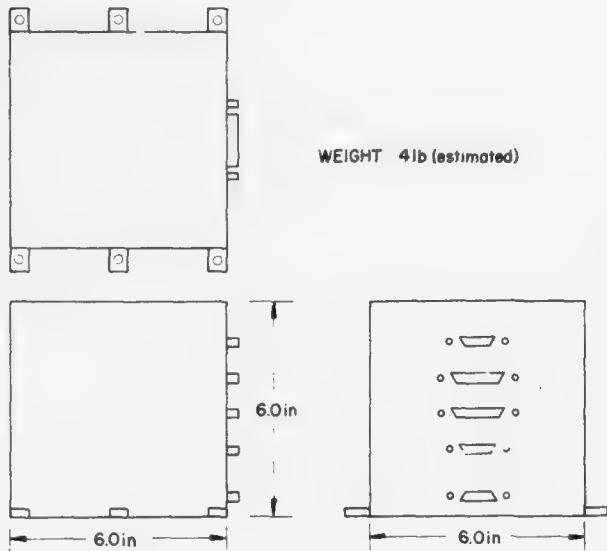
Figure 2-6. Electronics Package

SCATHA–THERMAL ELECTRON/ION MEASUREMENTS EXPERIMENT
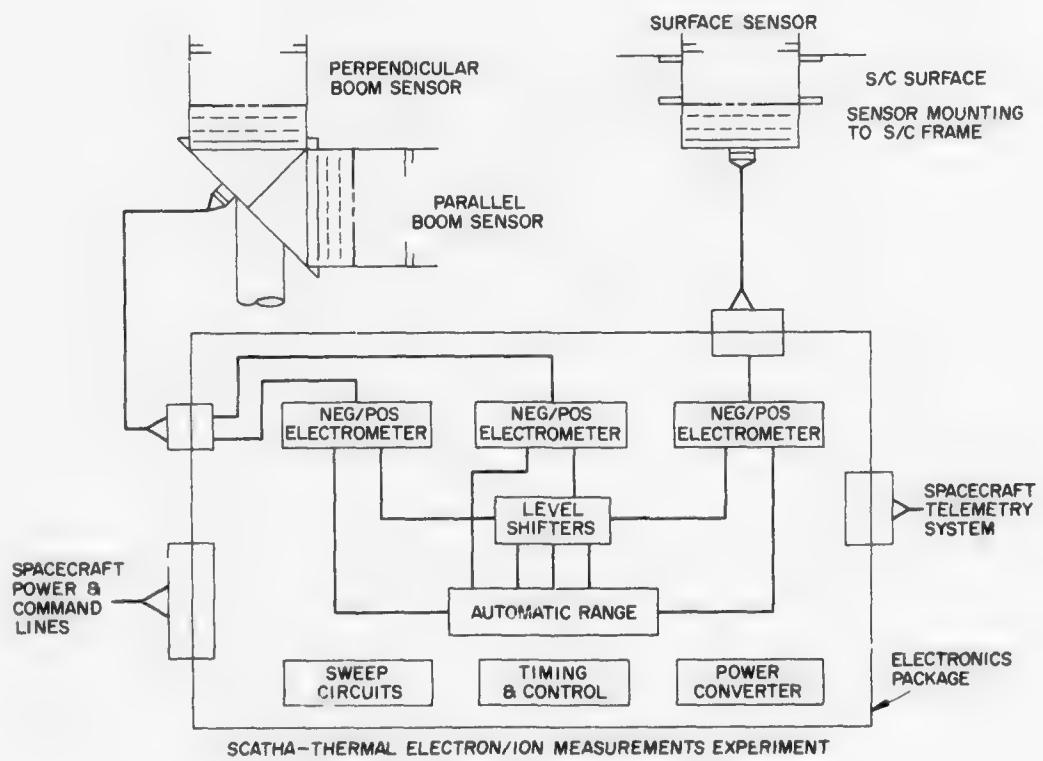
Figure 2-7. System Block Diagram

16

2.3 ELECTROMETERS

The linear range switching electrometers (Figure 2-8) are current to voltage amplifiers designed to have an output of 0 to 5V for each decade of input current. Each sensor's electrometer is programmed to measure either ions or electrons. The electrometer uses a MOSFET operational amplifier at the input to measure four decades of current over the range of 10^{-13} to 10^{-9}A. As the output voltage approaches 0 or 5V, the electrometer is automatically switched into the next current range. Internal calibration signals are applied to the electrometer input in each range approximately once every hour.
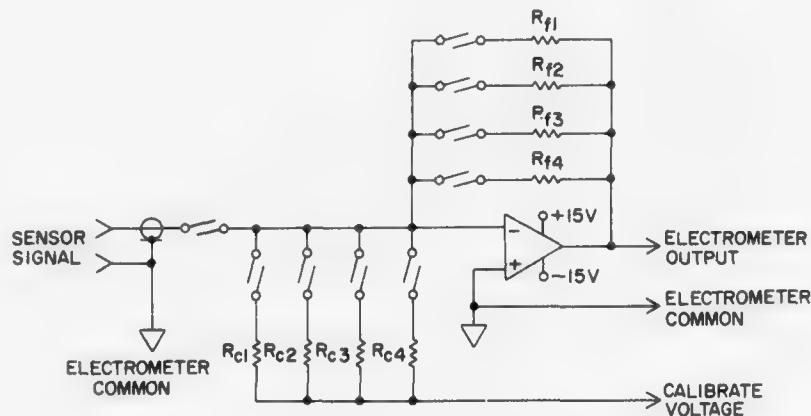
Figure 2-8. Electrometer Circuit

Because extremely high values of feedback resistors (R_F) are necessary, the electrometer circuits tend to be temperature dependent. Therefore, a separate temperature monitor (thermistor) is provided for each electrometer. These outputs will be used to determine in-flight amplifier characteristics based on pre-flight laboratory temperature calibrations and testing.

To achieve the various operation modes of the experiment, several fixed and varying voltage signals must be periodically applied to the electrometer common and sensor elements. To do this, the electrometer common must be electrically floating with respect to the system common or spacecraft ground. Since the electrometer output voltage is consequently "riding on" the varying signals being applied to the electrometer common, a level shifter circuit must be employed to reference the 0- to 5-V output signal to system common.

17

2-4. LEVEL SHIFTERS

Each level shifter circuit is a differential operational amplifier which measures the difference between the electrometer common and the electrometer output. The electrometer common is floating with respect to telemetry common.

The level shifting is achieved by dividing the electrometer common and the electrometer output separately by 10, using the resistor divider networks as shown in Figure 2-9. Since the bias potentials on the electrometer may be as high as 120V this division is necessary to reduce these levels to within the maximum operating range of the operational amplifiers.
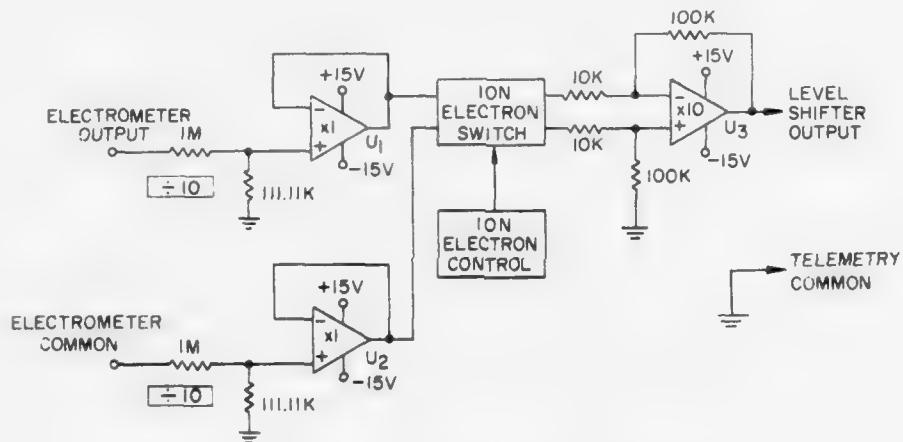
Figure 2-9.   Level Shifter Circuit

The reduced output levels are then impedance matched through the voltage follower circuits U_1 and U_2 and applied to the input of the differential operational amplifier U_3, which amplifies the difference of the two signals by 10. Located between U_1, U_2, and U_3 is a switching arrangement to adjust for polarity differences between ion and electron signals. The output of U_3, which is referenced to circuit common, is sent to the spacecraft data transmittal system and to the automatic range-switching circuit.

18

2-5. AUTOMATIC RANGE-SWITCHING CIRCUITS

The output of the level shifter is connected to a comparator circuit which com-
mands the range-switch circuit (Figure 2-10) to either step the electrometer up or
down into a new sensitivity range. This happens whenever the level shifter output
signal goes below 350 mV or above 5.0V.

The up/down command line has a 100 msec delay network to filter out noise.
After a positive command has been established, an up/down counter is advanced by
one count. The counter has a Binary Coded Decimal (BCD) output which is decoded
to operate reed relays in the electrometer. These relays are in the resistor feed-
back loop and control the current to voltage relationship. The BCD outputs are also
used to control the range monitor output voltage levels. The up/down counter is
periodically jammed with a code for controlling the calibration of the electrometer.
During this mode, the range-switch circuit is inhibited.
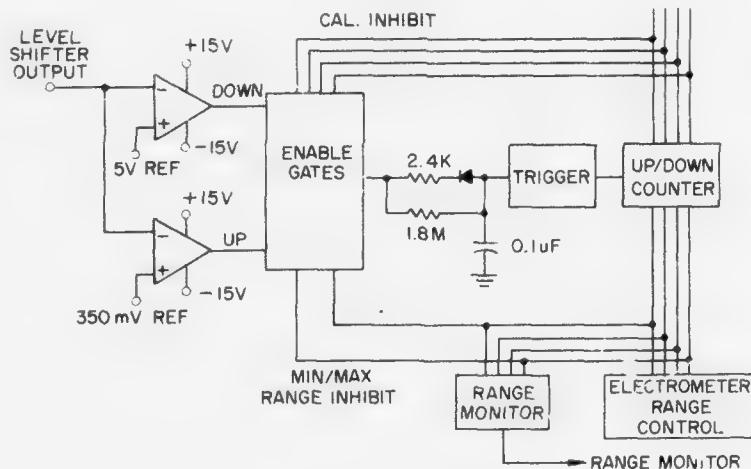
Figure 2-10. Automatic Range-Switching Circuit

2-6. STEP GENERATOR

Two step generators (ion and electron) are used for stepping the sensor grid
elements and the electrometer floating common. One generator is applied during
ion modes and the other is applied in the electron modes.

2-7. TIMING AND CONTROL CIRCUITS

Timing of the system program is clocked from a spacecraft provided 1-Hz pulse. The system program cycle is approximately 1 hour long. The cycle is achieved by using a 12-stage counter and a diode matrix. The decoded lines from the matrix are used for controlling the electrometer calibration sequence and sweep periods. The system timed sequence of events is shown in Figure 2-11.

CAL. CYCLE – INTERNAL ELECTROMETER CALIBRATION ON EACH OF THE FOUR RANGES
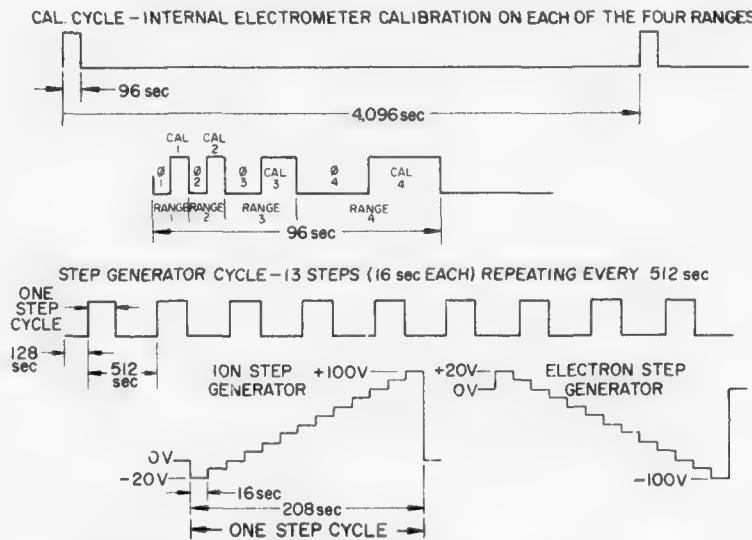
Figure 2-11. System Timed Sequence of Events

2.8 DC-DC POWER CONVERTER

The various voltages required for the experiment circuits are provided from a multiple output voltage dc-dc power converter operating off of the spacecraft +28 V power system. The converter chopper frequency is 25 kHz ± 5 kHz. All of the secondary experiment voltages are regulated and current limited.

2-9. TELEMETRY OUTPUTS

The experiment data output lines are listed below. Each output is fed to a telemetry system consisting of an 8-bit Analog/Digital Converter and a Pulse Coded Modulation (PCM) encoder.

20

Table 2-1. Data Output Lines

TM Output Description	Type	Bandwidth or Sample Rate	Bits/sec
Current Sensor 1A	Analog	8/sec	64
Range/Cal Sensor 1A	Analog	8/sec	64
Current Sensor 1R	Analog	8/sec	64
Range/Cal Sensor 1R	Analog	8/sec	64
Current Sensor 2	Analog	8/sec	64
Range/Cal Sensor 2	Analog	8/sec	64
Step Monitor	Analog	8/sec	64
Event Monitor	Analog	2/sec	16
Temp Monitor 1A	Analog	.25/sec	2
Temp Monitor 1R	Analog	.25/sec	2
Temp Monitor 2	Analog	.25/sec	2
Bias Monitor	Analog	0.0625/sec	0.5

*These output words to be contiguous in the telemetry format.

Contents

3. Rapid Scan Particle Detector

A. Pavel, Capt, USAF, L. Katz, P. Rothwell
Air Force Geophysics Laboratory
Hanscom AFB, Massachusetts
B. Sellars, F. Hanser, P. Morel, J. Hunerwadel
Panametrics, Inc.
Waltham, Massachusetts

3-1. INTRODUCTION

The Rapid Scan Particle Detector is a high time-resolution particle spectrometer designed to measure magnetospheric substorm particle fluxes at synchronous orbit under spacecraft charging conditions. The rapid time analysis of particle fluxes is essential to an understanding of transient spacecraft charging effects and the damaging currents and arcing that can occur during their events. This instrument has been designed to provide rapid time analysis for the interpretation of engineering experiments and during operation of the electron and positive-ion beam systems. One second complete spectral resolution will be possible, with the capability of submillisecond resolution on selected energy channels. High time resolution is accomplished with several wide acceptance cone detectors. Figure 3-1 shows some flight detectors prior to assembly. A total of 12 detectors are contained in the one Rapid Scan Particle Detector package. Electrostatic Analyzers (ESA's) are in the upper portion of Figure 3-1 and Solid State Spectrometers (SSS's) are in the lower portion.
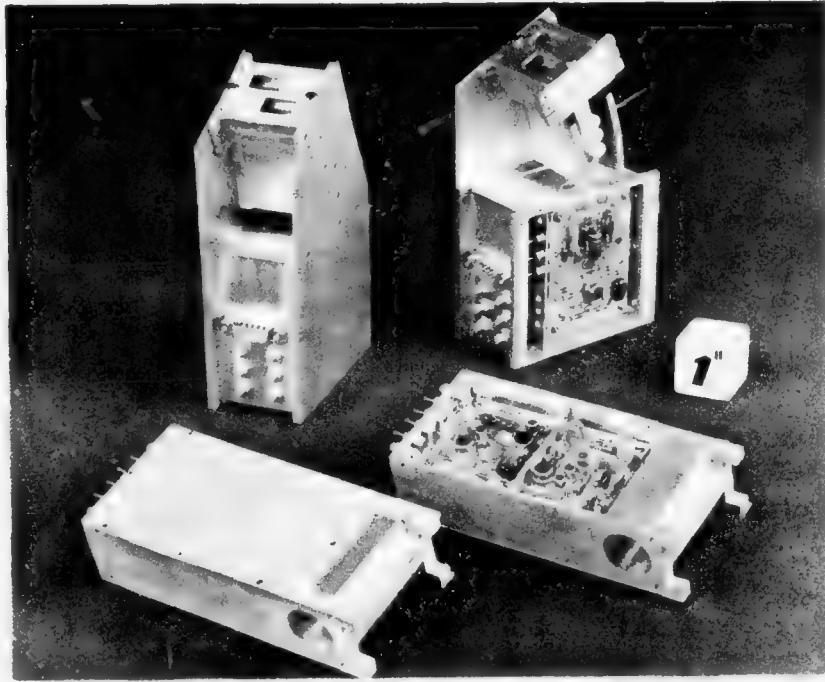
Figure 3-1. Flight Components of the Rapid Scan Particle Detector. Electrostatic analyzers are in upper portion of figure and solid state spectrometers in lower portion. A total of 12 sensors will be assembled in one package

The Rapid Scan Particle Detector will perform a differential energy analysis of 50 eV to 10 MeV electrons and 50 eV to 35 MeV protons. This is accomplished by using low energy ESA's to cover the 50 eV to 1.7 keV range, high energy ESA's to cover the 1.7 to 60 keV range, and solid state spectrometers for measurements above that. Two complete sets of detectors are used, one of which is to be oriented perpendicular to the satellite spin axis and the other parallel to the spin axis. A simplified instrument block diagram is shown in Figure 3-2 and an instrument outline drawing in Figure 3-3.

This instrument has a volume of 864 in.^{3} (0.5 ft^3) and weighs about 13 lb. An examination of Figure 3-2 indicates that the instrument can be readily divided into seven major subsystems as follows:

(1) Four Electrostatic Analyzers (ESA's) which measure low energy electrons and protons.

(2) Four Solid State Spectrometers (SSS's) which measure higher energy electrons and protons.

24
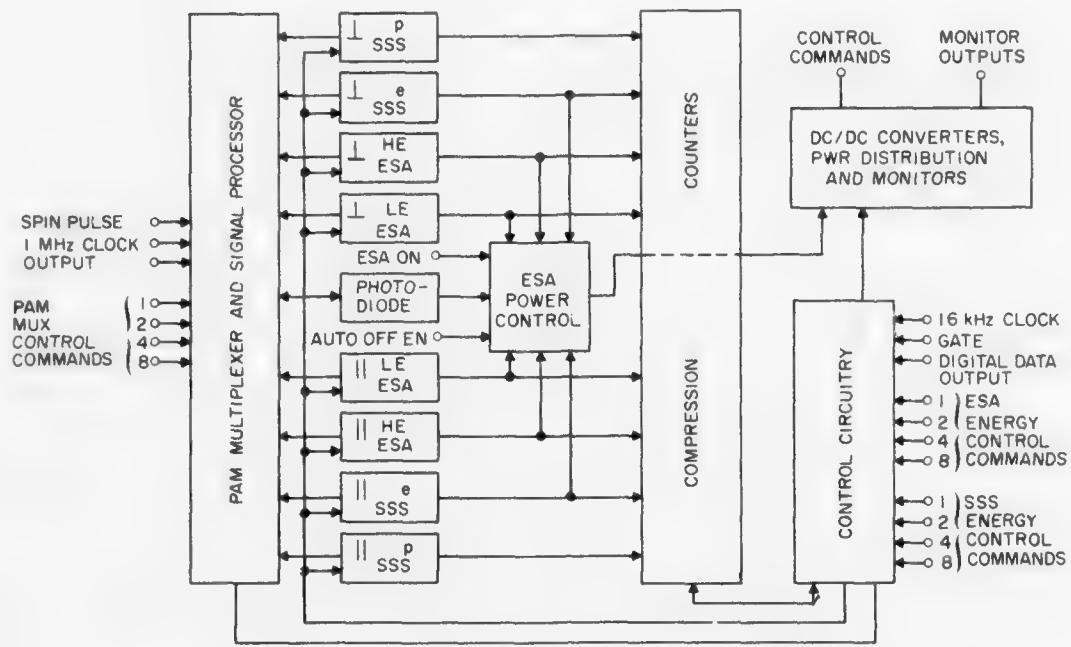
Figure 3-2. Simplified Instrument Block Diagram

(3) The compression counters which accumulate the pulses from the ESA's and SSS's and compress the information so as to minimize the instrument's telemetry requirements.

(4) The PAM multiplexer and signal processing circuitry which is assigned to a particular ESA or SSS, by ground command, and provides a very high time-resolution monitor of its activity.

(5) The control circuitry which allows for completely independent control of ESA and SSS energy channel sweep rate or assignment, via ground command. This subsystem also controls the transfer of digital data from the instrument to the satellite data handling system.

(6) The electrostatic analyzer power control circuitry which automatically shuts off the ESA's when the flux level exceeds certain predetermined levels and would result in premature Channeltron electron multiplier gain degradation.

(7) The dc to dc converter, power distribution, and monitors subsystem, which contains all the required high voltage power supplies, dc to dc converters and analog voltage and temperature monitors.

25

NOTES:

1▷ REQUIRED FIELD OF VIEW ⊥ TO SPIN AXIS. BORESIGHT ⊥ TO SURFACE WHICH IS ⊥ TO BASEPLATE AND ‖ TO BOLT HOLE REFERENCE LINE.

2▷ REQUIRED FIELD OF VIEW ‖ TO SPIN AXIS. BORESIGHT ⊥ TO BASEPLATE.

MATING CONNECTOR

BENDIX RF CONNECTOR

TEST CONNECTOR TBD
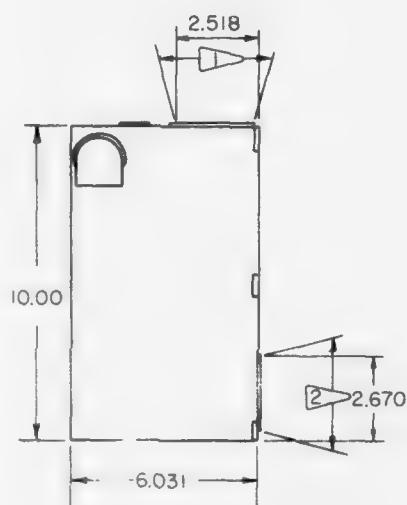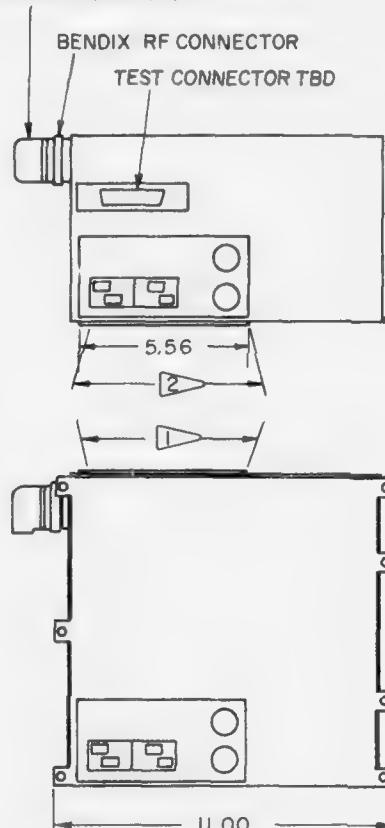
Figure 3-3. Outline Drawing

A detailed discussion of these subsystems is contained in the following sub-sections.

3.2 ELECTROSTATIC ANALYZERS

A simplified block diagram of the Electrostatic Analyzer (ESA) subassembly is shown in Figure 3-4. Energy analysis is accomplished by a three-plate cylindrical electrostatic analyzer with the outer plates grounded and a programmed, negative deflection voltage applied to the inner plate. Electrons are analyzed by the inner plates while protons are simultaneously analyzed by the outer plates—in both cases selected particles are detected by a Spiraltron Electron Multiplier (SEM).

26
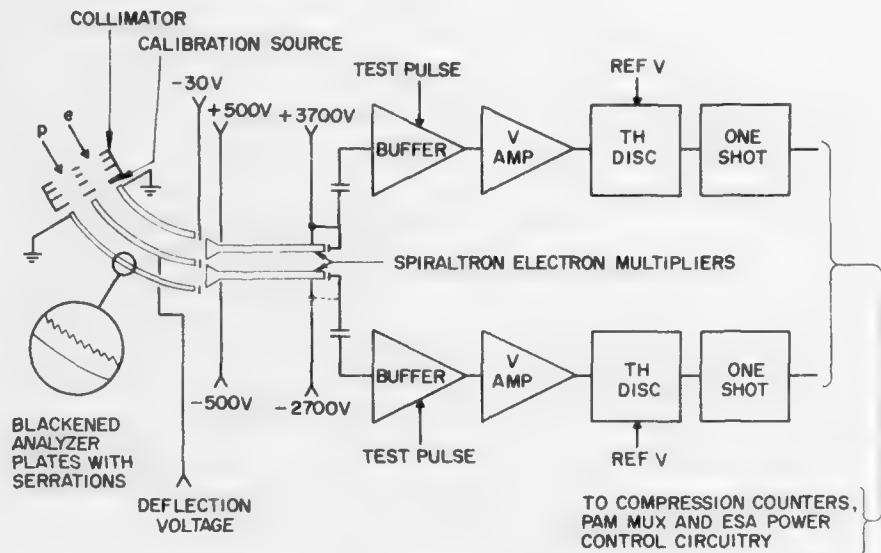
Figure 3-4. Electrostatic Analyzers

The front end of the electron SEM is biased at +500V to accelerate low energy electrons, thereby obtaining better detection efficiency. This requires the output end of the SEM be biased at +3500V to obtain a nominal operating voltage of 3000V. Similarly, the front end of the proton SEM is biased at -500V, requiring its output end to be biased at +2500V. These bias voltages are nominal levels, the actual set of bias levels being one of four possible sets, as selected by two ground commands. This arrangement allows the SEM's to be biased initially at fairly low voltages (low gain) and to increase the bias voltages (and gains) if gain fatigue is experienced. An additional benefit is that fatigue is delayed, since it is a function of the charge removed from the SEM, not the total accumulated counts. Thus, the total life in terms of accumulated counts is actually extended. A suppression grid biased at -30V is placed between the deflection plates and the electron SEM to inhibit the detection of secondary electrons emitted by the deflection plates.

Each SEM drives a Buffer Amplifier, Voltage Amplifier, Threshold Discriminator, One Shot chain. The input to the high impedance unity gain buffer is protected from damage due to corona or high voltage breakdown in the SEM or deflection plates. The voltage amplifier gain and threshold discriminator firing level are such that nominal SEM gain variations can be tolerated. The threshold discriminator output is fed to a one shot which generates a logic level pulse of fixed duration and drives the compression counter, PAM multiplexer, and ESA power control circuitry.

27

A single test pulse is injected into the buffer amplifier input during each data accumulation interval, thus ascertaining proper operation of the signal processing circuitry. A low intensity conversion electron source is also included in front of the electron anaylzer to further verify proper system performance. The source intensity will be sufficiently low that it will not interfere with spectrum determination during substorms.

Four ESA subassemblies are included within the instrument. Two low energy (LE) units each cover the 0.05- to 1.7-keV energy range, while two high energy (HE) units simultaneously cover the 1.7- to 60-keV energy range. These are oriented such that two (one LE and one HE) look perpendicular to the satellite spin axis and the other two look parallel to that axis.

Each ESA's energy range is covered in 4 increments, as shown in Table 3-1. A background measurement is also included yielding a total of 5 ESA energy channels. Data are accumulated and read out in 200-msec blocks, thus a complete ESA sweep (5 energy channels) can be completed in 1 sec. A command system is included which allows the ESA's to remain in the same energy channel for a number (up to 1024) of 200-msec data blocks, or to be fixed in a particular energy channel.

It should be noted that 8 ESA measurements are made simultaneously: $\perp$ LE e, $\perp$ LE p, $\parallel$ LE e, $\parallel$ LE p, $\perp$ HE e, $\perp$ HE p, $\parallel$ HE e, $\parallel$ HE p. Any one of these may be assigned to the high time-resolution PAM signal processor, via ground command.

Table 3-1. ESA Energy Detection Ranges

ESA Energy Channel	Energy Detection Ranges (keV)	
	Low Energy ESA	High Energy ESA
0	background	background
1	0.05 to 0.12	1.70 to 4.20
2	0.12 to 0.30	4.20 to 10.2
3	0.30 to 0.70	10.2 to 25.0
4	0.70 to 1.70	25.0 to 60.0

3-3. SOLID STATE SPECTROMETERS

A block diagram of the Solid State Spectrometer (SSS) subassembly is shown in Figure 3-5. Energy analysis is accomplished by a totally depleted silicon surface

28

barrier solid state detector (SSD), which produces a charge pulse proportional to the incident particle's energy. The Low Noise Charge Sensitive Preamplifier (CSPA) converts this charge pulse into a voltage pulse which is further amplified and fed to the threshold discriminators.

The threshold discriminator outputs drive one shots (OS) which generate logic level output pulses of fixed duration. These are combined by the window logic such that an output is obtained if, and only if, the lower level threshold is exceeded and the upper level threshold is not exceeded. The rear SSD determines whether the incident particle has penetrated the front detector. Simultaneous anticoincidence ($\overline{\text{COINC}}$) low energy, nonpenetrating, and coincidence (COINC) high energy, penetrating measurements are made and directed to the compression counters and PAM multiplexer circuitry.

A single test pulse is injected into the CSPA input during each data accumulation interval, thus ascertaining proper operation of the signal processing circuitry. A low intensity calibration source is also included to further verify proper system performance. The source intensity will be sufficiently low that it will not interfere with spectrum determination during substorms.
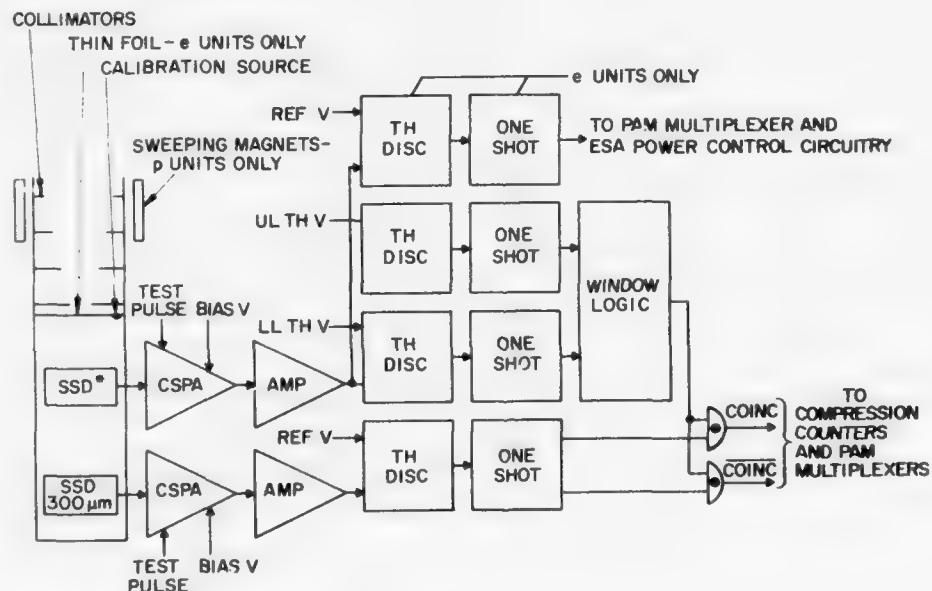

Figure 3-5. Solid State Spectrometer

The electron and proton SSS subassemblies are very similar, the only differences being:

(1) The front solid state detectors – the electron SSS front detector is 50 mm^2, 300 μm totally depleted whereas a 25 mm^2, 10μm totally depleted detector is used in the proton units. The rear detectors are all 100 mm^2, 300 μm partially depleted.

(2) The calibration sources used – Sn^{119} is used in the electron units while Am^{241}, degraded by a nickel foil, is used in the proton units.

(3) A thin foil is used in front of the electron units for the elimination of low energy protons.

(4) Sweeping magnets are used in front of the proton units for the elimination of low energy electrons. The use of a very thin detector in this assembly simplifies this problem in that only electrons with energies up to about 40 ke V need be eliminated. Higher energy electrons will pass through the detector and not deposit enough energy to cause a false count.

(5) The electron SSS contains an additional fixed threshold discriminator and one shot, which are used to activate the automatic ESA power shutdown circuitry during periods of excessively high electron flux levels.

Four SSS subassemblies are included within the instrument, two electron units each covering the 30- to 10,000-ke V energy range and two proton units each covering the 70- to 35,000 ke V energy range. These are oriented the same as the ESA's – two (one electron and one proton) look perpendicular to the satellite spin axis and the other two look parallel to that axis.

As in the case of the ESA's, there are 5 SSS energy channels. Since two measurements are made simultaneously ($\overline{\text{COINC}}$ and COINC) a total of 10 measurements are made over the energy ranges, as shown in Table 3-2. Since data are accumulated and read out in 200-msec blocks, a complete energy spectrum can be generated in 1 sec. A command system is included which allows the SSS's to remain in the same energy channel for a number of 200-msec data blocks (up to 1024), or to be fixed in a particular energy channel. The command system allows complete independent control of the SSS and ESA energy channels.

It should be noted that 8 SSS measurements are made simultaneously – $\perp$e $\overline{\text{COINC}}$, $\perp$e COINC, $\perp$ p $\overline{\text{COINC}}$, $\perp$p COINC, $\|$ e $\overline{\text{COINC}}$, $\|$COINC, $\|$ p $\overline{\text{COINC}}$ and $\|$ p COINC. These may be subcommutated on the high time resolution PAM signal processor, under ground command.

30

Table 3-2. SSS Energy Detection Ranges

| SSS Energy Channel | Energy Detection Ranges (keV) | | | |
| | Electron SSS | | Proton SSS | |
	$\overline{\text{COINC}}$	COINC	$\overline{\text{COINC}}$	COINC
0	30 to 45	background	70 to 100	15,000 to 35,000
1	45 to 70	background	100 to 165	6000 to 15,000
2	70 to 120	560 to 10,000	165 to 290	2400 to 6000
3	120 to 170	275 to 560	290 to 450	1200 to 2400
4	170 to 243	243 to 275	450 to 725	725 to 1200

3-4. INSTRUMENT CALIBRATION

The geometric factors of the SSS's can be calculated quite readily from the collimator dimensions, and checked with measurements on calibrated particle sources. The ESA geometric factors are more difficult to determine. The transmission characteristics of the cylindrical plate ESA's are calculable, but the effect of fringing fields and internal scattering introduces uncertainty into these calculations. Finally, the efficiency of the Spiraltrons is not unity, as is the case with solid state detectors, and varies across the face of the funnel. Thus, the ESA's will undergo a thorough calibration procedure using electron sources. The entire procedure is not discussed here, but the results of some tests on the Spiraltons are presented.

Tests of the relative response across the face of the Spiraltron have been performed. The test setup is shown in Figure 3-6, where the method of scanning the funnel area with a radioactive beta source (^{3}H or ^{63}Ni) is illustrated. The first test made was to check the shape of the relative detection efficiency for the funnel grounded, and at +500 V, the configuration to be used in the ESA's. The results are shown in Figure 3-7, where the effects of low energy ($\lesssim$ 30 eV) electrons are shown to be small by the V_R = 0 data being close to the V_R $\approx$ -30 V data. The results show that detection efficiency is maximum near the center of the funnel, and falls to zero near the edge. We also find that applying an accelerating potential narrows the area of maximum response, although for a ^{3}H spectrum (average energy $\approx$ 5 keV) the central response magnitude does not change very much.

31
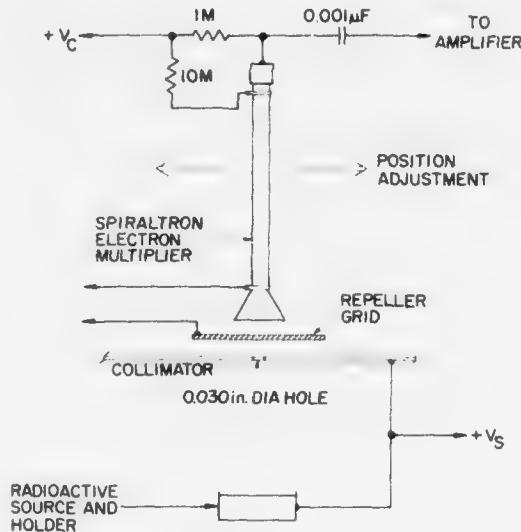
Figure 3-6. Test Setup for Efficiency Measurements of Spiralton Electron Multiplier
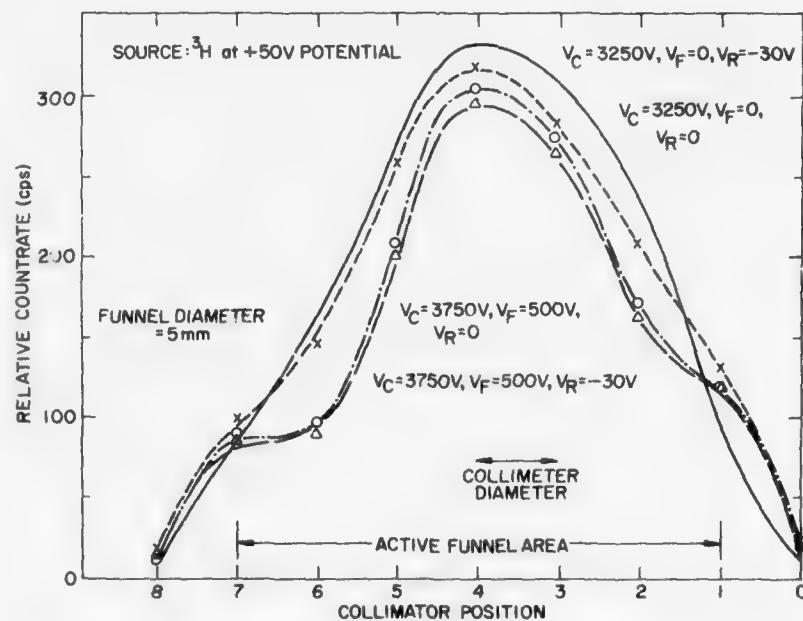
Figure 3-7. Spiraltron Electron Multiplier Relative Efficiency-Variation with Funnel Voltage

Figure 3-8 shows the relative Spiraltron efficiency profile for three different energy ranges, with a 500 V preacceleration potential on the funnel. For the uncovered ^{3}H source the average energy is about 5 ke V, for the ^{3}H source with 129 μg/cm^2 of polypropylene it is about 4 ke V, and for the ^{63}Ni source it is about 17 ke V. Within the position accuracy shown in Figure 3-8, there is no significant change in shape of the Spiraltron response. More refined tests of the type shown in Figures 3-7 and 3-8 are planned. In particular, a series of tests using mono-energetic electrons from a cylindrical plate analyzer will be carried out.
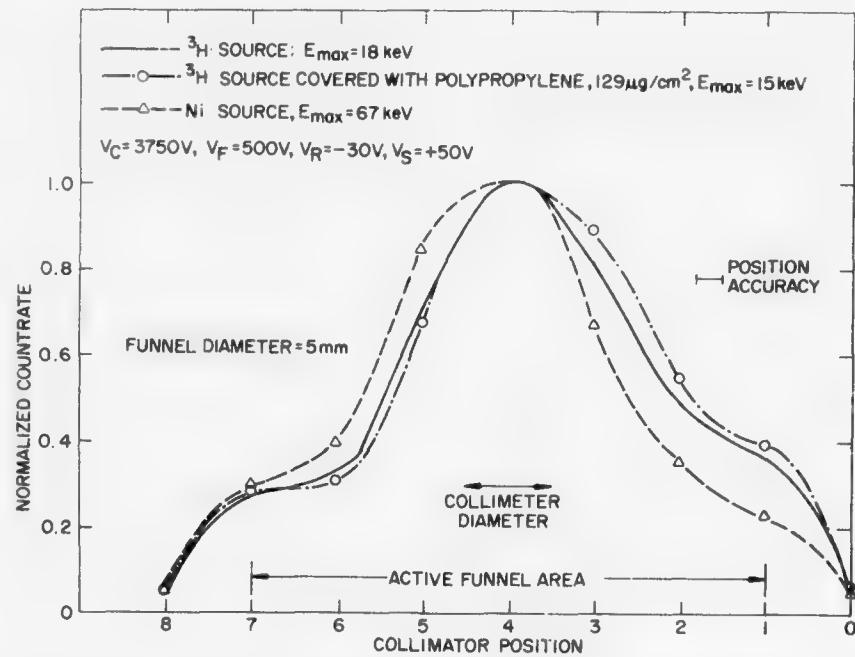
Figure 3-8. Spiraltron Electron Multiplier Normalized Efficiency-Variation with Electron Voltage

33

Contents

4. Electron Beam System

H. Cohen and W. Lynch
Air Force Geophysics Laboratory
Hanscom AFB, Massachusetts

4-1. INTRODUCTION

An Electron Beam System, consisting of an indirectly heated, oxide-coated cathode and a control grid, will function to control the ejection of negative charge (electrons) from the Space Vehicle. The cathode will be kept at a controlled negative potential with respect to the Space Vehicle. This potential will determine the energy of the ejected electrons, and will be controlled in steps from 50 to 3000 V by ground command. The control grid is normally kept negative with respect to the cathode, and is pulsed positively to allow electron ejection current. The duration and electron current level of the pulse is controlled by ground command. A focusing element between the control grid and the grounded exit anode serves to narrow the electron beam angular spread. Figure 4-1 shows the assembled Electron Beam System and Figure 4-2 depicts the Machlett Laboratories EE-65 electron gun around which the Electron Beam System has been designed.

The Electron Beam System is body mounted to the Space Vehicle and positioned with its beam axes perpendicular to the Space Vehicle spin axis. It is mounted in bonded electrical contact with the Space Vehicle structure/frame ground. No surfaces at high potentials are permitted in the vicinity of the beam's geometries. The

Preceding page blank

electron beam at energies $\geq$ 1.5 keV constitutes a conical region of influence of less than 3.5 deg half angle, and will not be permitted to impinge on other Space Vehicle or payload components.
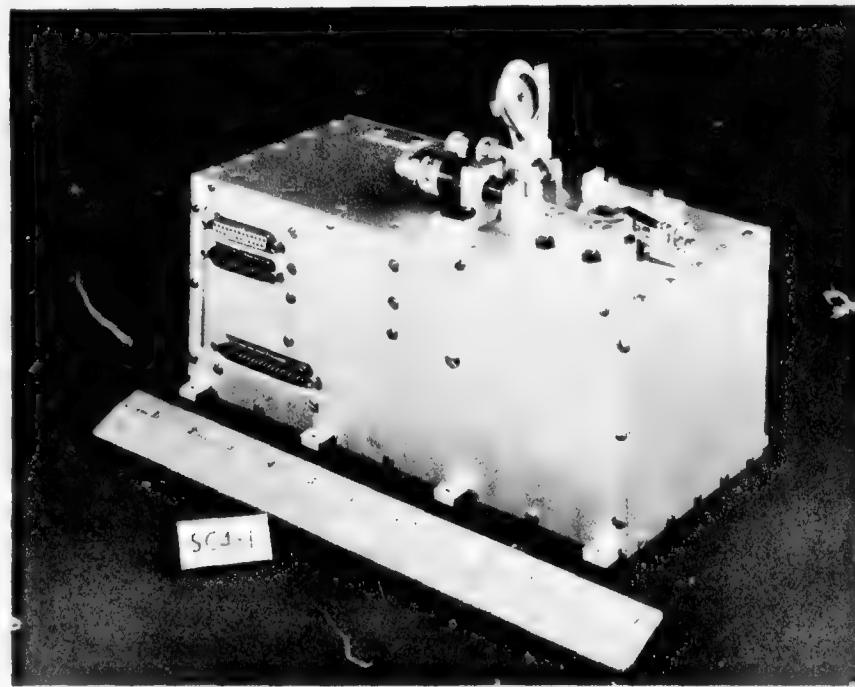
Figure 4-1. Assembled Electron Beam System Showing Cap Opened on Electron Gun
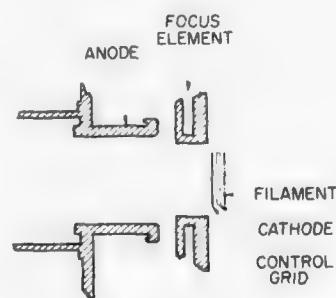
Figure 4-2. EE-65 Electron Gun

The Electron Beam Gun has an aperture sealed-cover mechanism which is opened on orbit by ground commanded squib firing. The cover then swings away from the aperture and is retained by the mechanisms. Figure 4-3 shows the outside configuration of the electron gun. Figure 4-4 is an exterior view of the entire Electron Beam System.
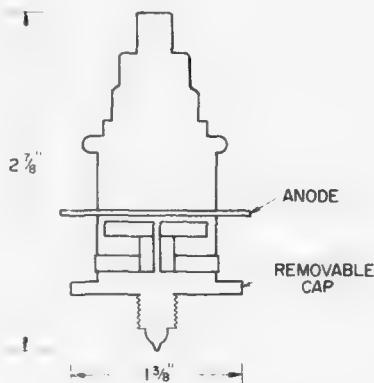
Figure 4-3. Electron Gun Configuration
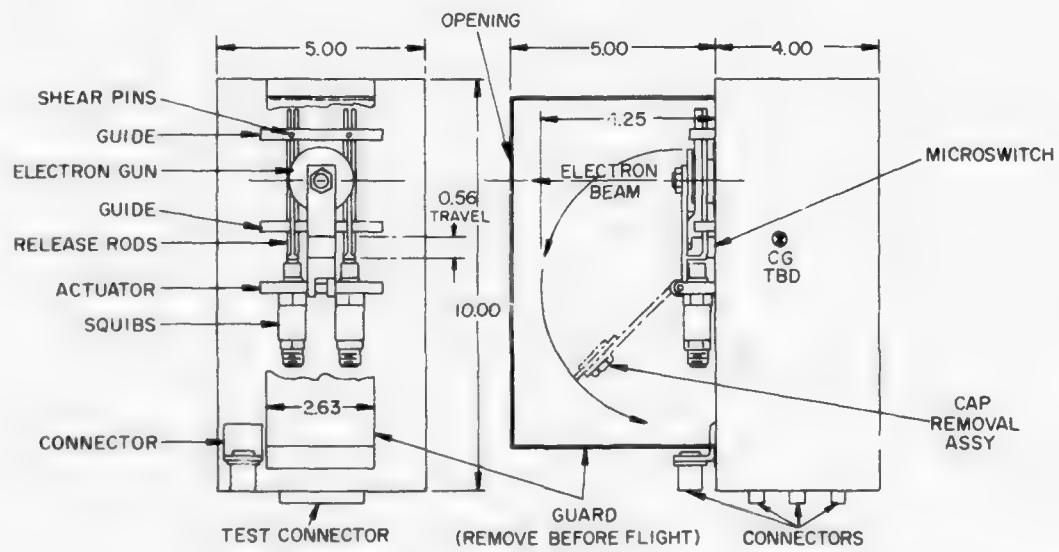
Figure 4-4. Electron Beam System Exterior

37

The removal of the aperture cover of the Electron gun is accomplished by ground command after achieving in-orbit operations. This removal requires the firing of redundant squibs (Holex No. 10257).

When the gun is on, but no beam is ejected, the average power drawn is 8.2 W. Beam ejection increases the power drawn according to the product of the beam current and accelerating voltage, both of which are commandable from the ground. There are six accelerating voltage steps and six current steps:

Accelerating Voltage (Vdc):   50,   150,   300,   500,   1500,   3000

Current (mA):   .001,   .01,   .1,   1.0,   6.0,   13

All combinations are possible except 3000 V at 13 mA. The maximum power drawn is 42 W for the combination 1500 V and 13 mA.

4-2. SYSTEM DESCRIPTION

The electron beam system is designed around the Machlett Laboratories EE65 electron gun. The system provides six beam energy levels, six peak beam current levels, two beam duty cycles and three focus ring voltage levels. These are selectable by command signals in any combination except that which exceeds 50 W on spacecraft input power.

4-2.1 Power Supply

A block diagram of the power supply is shown in Figure 4-5. The design model high voltage supply does not use a multiplier. The volume and weight of filter capacitors required for multiplier filter capacitors rated at 3000 V with a capacity capable of regulating with load from essentially zero current to 13 mA precludes their use.

The added versatility of beam energy levels below 500 V in anticipation of a new gun design from Machlett Laboratories requires an increase in range of energy control from 6 to 1 perhaps 60 to 1. The added versatility of focus ring variation requires the use of floating reed relays to switch the focus ring to taps on the high voltage divider.

Tests on the EE65 gun demonstrate that the grid drive state will require as much as +30 V at as much as 7 mA. Also, there is the possibility of a new gun design requiring in the order of -20 V to shut off the beam. These items require a floating beam control supply of seventy volts (± 35 V).

38
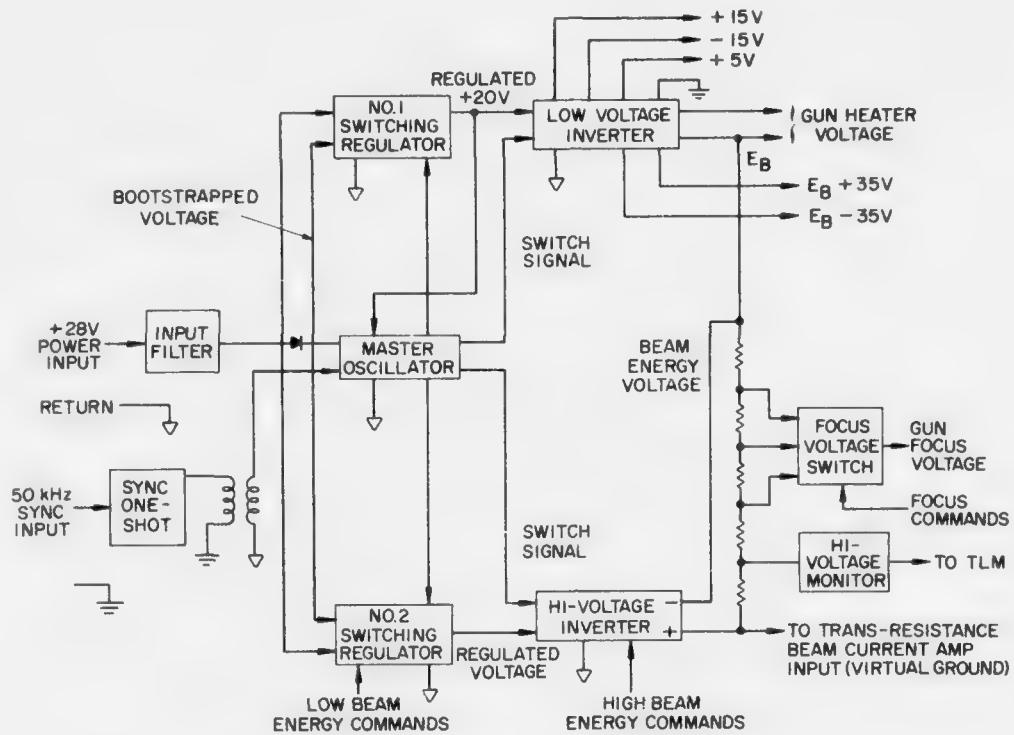
Figure 4-5. Power Supply

Referring to Figure 4-5, the input power lines contain an LC filter to reduce conducted emissions from the power supply switching regulators and inverters. The output of the filter powers two switching regulators; one for the high voltage inverter and the other for the low voltage inverter. The output of switching regulator No. 1 is 20 V referred to input power return. This regulated power feeds the master oscillator as well as the low voltage inverter.

The master oscillator provides a bootstrapped supply on top of the input +28 V so that both switching regulator pass transistors may be bottomed at low input line voltage and therefore, maintain high efficiency. The oscillator also provides dither signals for the switching regulators, and switch signals for both inverters. Thus the switching regulators and the inverters are all synchronized to the master oscillator.

The master oscillator is a low power ferrite core transformer type designed to free-run in the saturating mode at 20 kHz. It is synchronized by means of a TTL

compatible 50-kHz square wave from the spacecraft system. Signal coupling is accomplished by means of a small transformer in order to isolate the power ground from the signal ground return of the synchronizing signal.

The switching regulators are non-saturating. The switching transistor base drives are supplied by secondary windings on the master oscillator transformer.

Switching regulator No. 1 provides +5 V referred to signal ground for the TTL logic circuits, ± 15 V referred to signal ground for the analog circuits, an ac winding for the electron gun heater referred to negative high voltage, and a floating ± 35 V referred to negative high voltage for the electron gun control grid amplifier. Secondary series regulators, although not shown on the block diagram, are used for the ± 15-V analog circuit supply.

Switching regulator No. 2 powers the high voltage inverter. The inverter has one pair of switching transistors and five transformers with primary windings that are operated in parallel, and with secondary rectified supplies wired in series to develop the high voltage. The first three secondary supplies produce 500 V each and the last two produce 750 V each. As a function of the high beam energy commands, 1, 3, or 5 transformer primaries are switched into the inverter collector circuits producing 500 V, 1500 V, and 3000 V at the output of the stack of secondary supplies.

Those secondary supplies that are in the off state in other than the 3000 V mode essentially look like short circuits due to the forward biasing of the rectifier diodes. The input voltage from the switching regulator in the high beam energy mode is +20 V, referred to power return.

In the three low beam energy modes of 300 V, 150 V, and 50 V, a single 500 V secondary transformer is placed in the high voltage string, and the switching regulator output as a function of command signals is reduced to approximately 12 V, 4 V, and 2 V. This reduces the single secondary output to the required levels for the low energy modes.

A high impedance divider is placed across the high voltage to develop voltages for the focus anode of the gun and for the slow speed analog monitor to telemetry (TLM). The focus switches are small reed relays capable of 3000-V isolation between their contacts and their energizing coils which are driven from command circuits. The focus levels are 5%, 10%, and 20% of the high voltage tapped down from the negative high voltage.

The positive end of the supply is at a 0-V potential referred to signal ground but not connected to ground. This point is the input of a trans-resistance amplifier which monitors and controls the beam return currents, either from spacecraft skin return in flight or from the gun cap in test and before cap removal during flight. The TLM monitor of high voltage is a very high input impedance amplifier. Thus,

40

all bleeder current is returned to the power supply without being a part of the measured and controlled beam current.

Both switching regulators use a Schottky barrier diode for commutation at the input of the regulator inductors. This is an extremely fast device with an "on" voltage less than half that of a conventional silicon diode. This technique plus the use of the bootstrap voltage from the master oscillator provide a regulator efficiency of 90 percent at maximum secondary power. Breadboard tests confirm the design estimates.

It should be noted that the base drive for the high voltage inverter transistors is constant over the complete dynamic range of output voltage and load currents. This average power is 0.4 W.

4-2.2   Electron Gun Control Circuits

A block diagram of the Electron Gun Control Circuits is shown in Figure 4-6. The basic elements of the gun control circuits are: (1) a current to voltage amplifier A1, with command switched gain, (2) a strobed comparator amplifier A2, to compare the output of A1 with a low temperature coefficient reference voltage, (3) an optical isolator to transform the beam control signal to the high voltage level of the gun control grid, and (4) a floating grid driver amplifier A3. In addition, there is a 4.5 decade logarithmic electrometer to monitor the gun cap current.

When the beam is on, the control loop is such that the output of A1 is forced to the reference voltage of 6.4 V. Any error voltage between the output of A1 and the reference is amplified through A1, the optical isolator A3, and the gun. The gun beam current, either from the cap or from skin return current passes through the low voltage power supplies to the output of A1, and through the command selectable feedback resistor to the positive return of the beam energy supply. The loop therefore, holds the beam current to a value equal to the reference voltage divided by the feedback resistor. The beam may be pulsed by strobing the comparator amplifier off and thus forcing the gun control grid to maximum negative voltage. The control feedback resistors are selected to produce beam currents of 0.001, 0.01, 0.1, 1, 6, and 15 mA.

Note that the anode ring is returned to the virtual ground or the positive return of the beam energy supply. At low energies significant anode ring currents could be present, and if returned to signal ground could cause a substantial error in actual beam current leaving the gun.

Within the dynamic range of control grid voltage available (± 30 V with respect to cathode) the beam current is controlled within 2 percent.

41
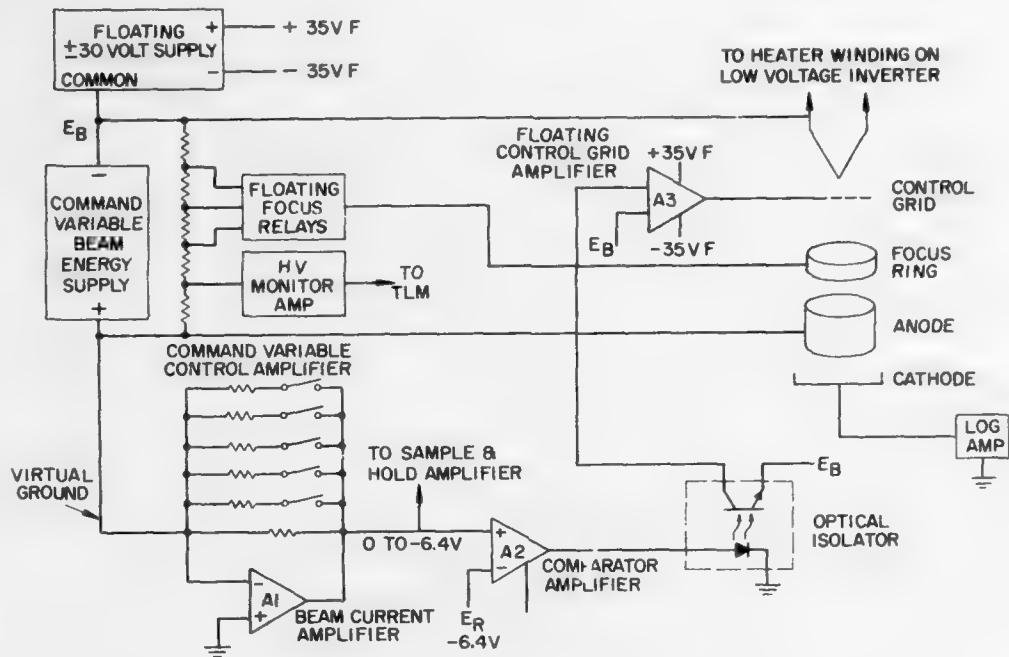
Figure 4-6. Electron Gun Control Circuits

4-2.3 Beam Current TLM Amplifiers

A block diagram of the Beam Current TLM Amplifiers is shown in Figure 4-7. The beam current amplifier output is sampled four times during one word length in the main frame. This is accomplished by gating and counting the PCM shift pulses during this word interval. The three stage counter output is decoded to produce 4 sample pulses, one word bit wide and spaced one word bit apart. During each sample period the output of the sample-and-hold amplifier follows the input.

When the timing signal goes low the output of the amplifier is held at the value of the input just prior to the timing signal change. The four outputs are presented to the TLM and are sampled at any 4 of the 128 words before the next sample-and-hold timing word.

In the pulsed mode one of the sixteen pulses per main frame (1/16 sec) are sampled four times during the pulse. The buffer amplifier between the beam current amplifier and the sample-and-hold amplifiers inverts the current amplifier and reduces it to +5 V full-scale.

42
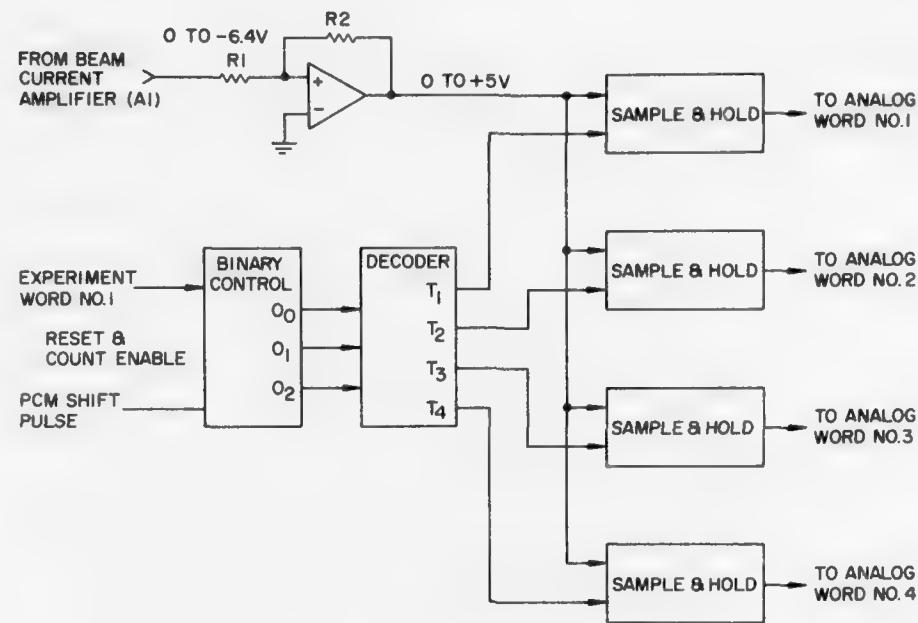
Figure 4-7. Beam Current Amplifiers

4-2.4 Auxiliary Circuits

In addition to those circuits shown in the block diagram there are 14 discrete flag outputs for command verification data, a pair of low voltage monitors, and a temperature monitor of the top plate of the box. The dynamic range of the temperature monitor is 0° to +70°C.

Contents

5. Positive Ion Beam System

H. Cohen and W. Lynch
Air Force Geophysics Laboratory
Hanscom AFB, Massachusetts

5-1. INTRODUCTION

A Positive Ion Beam System, consisting of a Penning discharge-chamber ion source and a control grid, will function to control the ejection of positive charge (xenon ions) from the Space Vehicle. A cylinder of pressurized xenon will consti- tute the gas source, controlled by a leak valve with the flow rate commandable from the ground. The duration and intensity of the ion beam are also controlled by ground command. Figure 5-1 shows the Positive Ion Beam System nozzle, a criti- cal element which will control the nature of the ejected xenon ion beam. The thin wires mounted on top are the beam neutralizers.

Beam ejection from the Positive Ion Beam System will be controlled in stepped voltage and current magnitudes by ground command. There are two beam bias voltages, 1000 Vdc and 2000 Vdc, and five current levels (0.3, 0.5, 1.0, 1.5, and 2.0 mA). The average power drawn when no beam is ejected is 14 W, and the maximum power drawn is 60 W during maximum beam ejection.

The Positive Ion Beam System will be body mounted to the Space Vehicle. It will be mounted in bonded electrical contact with the Space Vehicle structure/frame ground. No surfaces at high potentials are permitted in the vicinity of the beam's geometry. There is one pyrotechnic device associated with the Positive Ion Beam

45

Preceding page blank

System which is fired upon ground command after achieving on-orbit operations. A solenoid gas valve requiring 1A of current for 100 msec will control xenon gas flow to the Penning discharge chamber.
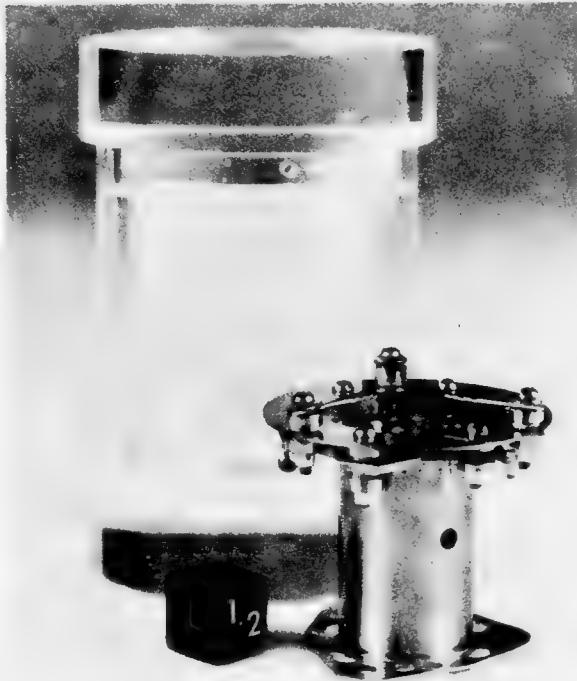
Figure 5-1. Nozzle Assembly for the Positive Ion Beam System. This critical element will control the nature of the ejected xenon ion beam

5-2. SYSTEM DESIGN

A block diagram of the Positive Ion Beam System design is shown in Figure 5-2, indicating the ion source, an expellant storage tank, a power processor, and a structural package. The ion source is packaged within a vacuum-tight enclosure having a cover that can be released by an electro-explosive device. Power obtained from a solar array and battery system in the spacecraft is processed to meet ion source, propellant valve, transducer, and telemetry requirements.

Positive ions extracted from a Penning-type discharge plasma are accelerated to high velocity electrostatically. In the discharge plasma, these ions are formed by collisions between atoms and electrons. A conventional hollow cathode is used to generate electrons which are then accelerated into the plasma by means of the discharge voltage. An axial magnetic field is used to restrict electron flow radially

46

and increase electron-atom collisions. Downstream of the ion accelerating grids is a neutralizer in the form of redundant thermionically emitting filaments. Depending upon the satellite experiment requirements, the neutralizer could be used to neutralize all or a fraction (including zero) of the ion beam.
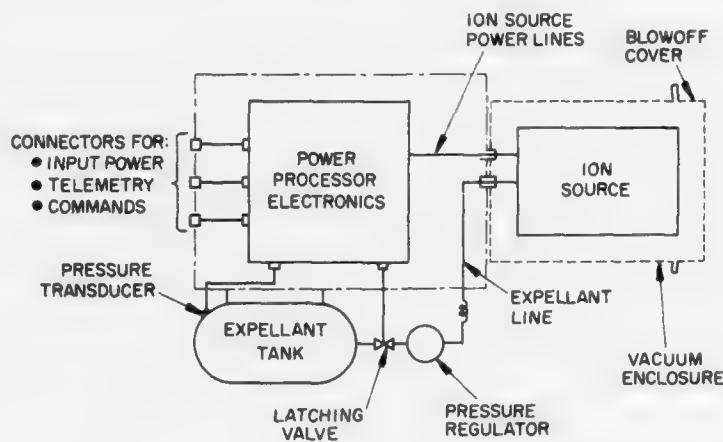

Figure 5-2. Satellite Positive Ion Beam System Block Diagram

The expellant storage tank is connected to the ion source through a pressure regulator, a solenoid operated latching valve, a porous plug, and an isolator. The ion source body is operated at high voltage and the propellant tank and valve are at ground potential with a ceramic "isolator" in the gas feedline. This grounding is used to minimize components and instrumentation (transducer) floating at high voltage.

5-3. SUMMARY OF THE ION BEAM SYSTEM CHARACTERISTICS

The Satellite Positive Ion Beam System is illustrated in Figure 5-3. The rectangular package configuration was selected over others, such as cylinders, because it provides for simple and convenient packaging, simple construction, and a large area near the power processor for heat rejection.

The ion source can be maintained under vacuum during storage and be exposed in space by releasing the blowoff cover. The blowoff cover also provides for preflight ground testing by removal of an O-ring-sealed plug in the pumpout port to allow evaluation. An ion collector mounted on the cover will indicate ion beam extraction.

47
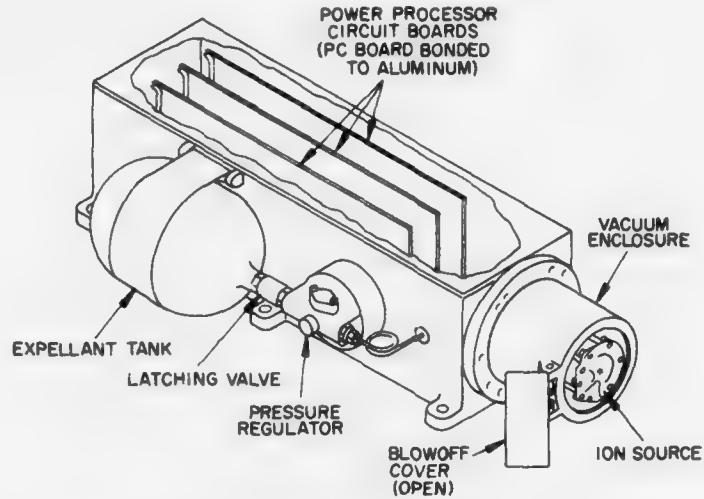
Figure 5-3. Isometric Sketch of Satellite Positive Ion
Beam System

5-4. ION BEAM SYSTEM DESCRIPTION

An assembly drawing of the proposed ion beam system is presented in Figure
5-4. The package overall dimensions are approximately 49 cm × 23 cm × 13 cm.
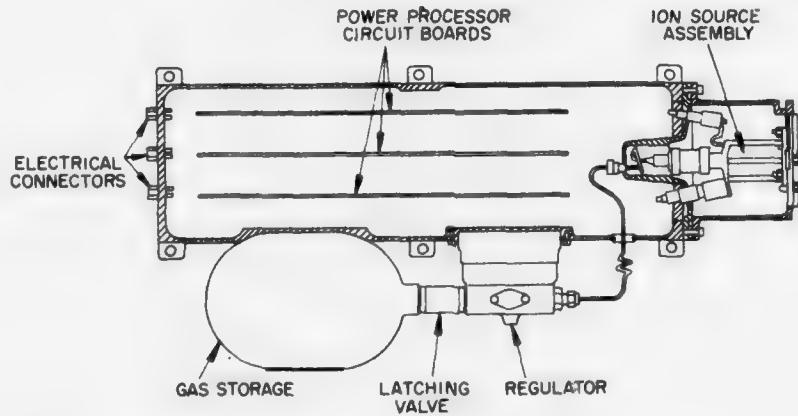
Figure 5-4. Ion Beam System Assembly Drawing

The major parts of the ion beam system include

(1) Ion Source Assembly:
   Ion source, Vacuum tight enclosure, Blowoff cover, Magnetic shielding,
   Pressure relief, Pumpout port.

(2) Expellant Assembly:
   Gas storage, Fill valve, Latching valve, Pressure regulator, Flow
   impedance, Pressure transducer.

(3) Power Processor Assembly:
   Power supplies for ion source, Power supply for valve, Power supplies
   for pressure transducer and temperature sensor, Command interface,
   Telemetry buffering, Temperature sensor.

(4) Structural Package
   Spacecraft interface (mechanical and thermal), Removable cover on
   electronics box, Vacuum tight interface with ion source.

A functional block diagram of the ion source and power processor is shown in
Figure 5-5. This diagram indicates the current paths (direction of ion flow) through
the various power supplies and the proposed grounding scheme. The decelerator
grid (to be operated at spacecraft potential) lead wire will be attached to the space-
craft "single point ground."

The power supply requirements imposed by the ion source assembly are pre-
sented in Table 5-1. These requirements include certain startup levels, five beam
power levels, power supply floating voltage relative to spacecraft ground, regula-
tion, ripple, and output control range. Although the data in Table 1 define the
power supply design requirements, additional information is needed to define the
input power profile during startup.

The electrical interfaces between the ion beam system assemblies and the
satellite subsystems are illustrated in Figure 5-6. The interconnections between
the ion source and the power processor are consistent with Figure 5-5. Note,
however, that a portion of the power supply outputs are "commoned" at the power
processor to reduce the number of vacuum terminals. The vacuum interface is
required to allow the ion source assembly to be evacuated during certain ground
tests. Figure 5-6 also indicates the method proposed for connecting command,
control signal, and analog returns.
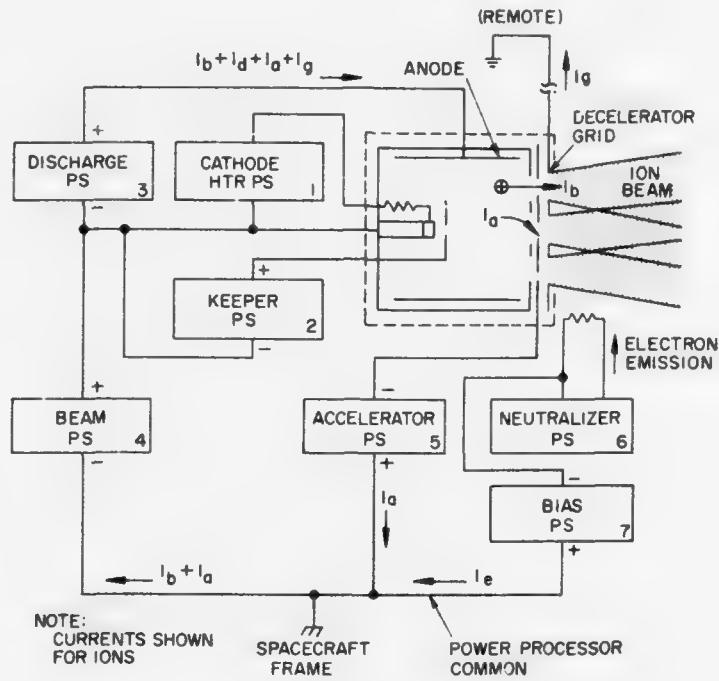
Figure 5-5. Functional Block Diagram of Ion Source and Power Processor

The power processor operates from a single voltage input in the range of 24 to 32 Vdc. This input is processed by a line regulator to provide regulated power (21 V) to an ac distribution inverter. Square wave (25 kHz, 42 V rms) ac power is delivered to each of the saturable reactor power supplies.

The command capability proposed for the present design is shown in Table 5-2. Although most of the commands are self-explanatory, a few commands require a brief explanation. The "instrument on" command provides telemetry buffering power and allows pressure, temperature, and inverter operation to be monitored and the gas valves to be opened. "Instrument off" turns off all power to the system. "Ion gun power on" and "off" operates a relay between the ac inverter and the various power supplies. Table 5-3 lists the analog output monitors for the Positive Ion Beam System.

Table 5-1. Power Supply Requirements

Power Supply No.	Power Supply Name	Type	Maximum Voltage Relative to S/C GND, V	Maximum Power		Typical Power		Regulation ±%	Range of Control
				Current, A	Voltage, V	Current, A	Voltage, V		
1	Cathode Heater	AC	+2500	5	6	3	3	Loop	1.0 to 5.0 (I)
2	Cathode Keeper	DC	+2500	0.2	25*	0.1	18	5 (I)	0.05 to 0.2 (I)
3	Discharge	DC	+2500	0.15	40	5×10^{-2}	25	5 (I)	0.01 to 0.15 (I)
4	Beam	DC	0	3×10^{-3}	2500	1×10^{-3}	1000	5 (V)	1000 to 2500 (V)
5	Accelerator	DC	0	1×10^{-3}	300	2×10^{-5}	300	5 (V)	100 to 300 (V)
6	Neutralizer Heater	AC	±1000	3	2	2.5	1.5	2 (I)	10 to 30 (I)
7	Neutralizer Bias	±DC	0	3×10^{-3}	1000	1×10^{-3}	0	5 (V)	0 to 1000 (V)

*1000 V open circuit

51
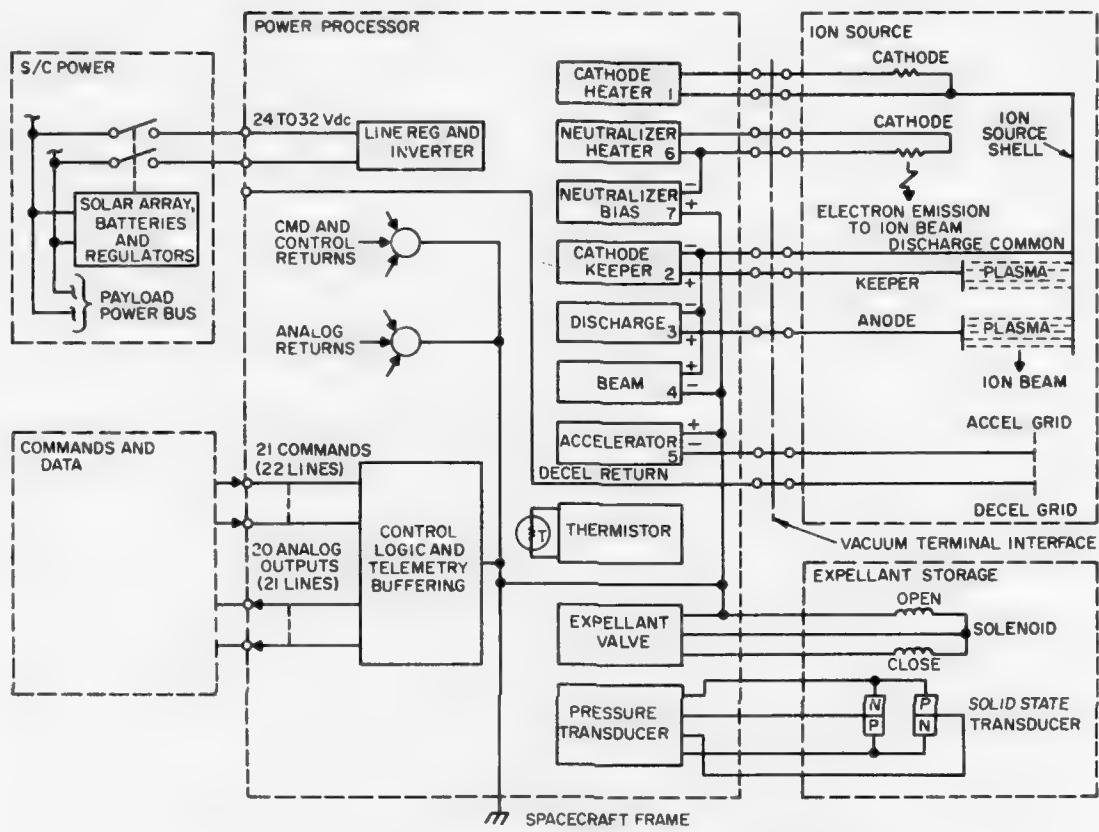
Figure 5-6. Ion Beam System Interface

Table 5-2. Command Capability

	Command	Function
1.	Instrument on	Turns on instrument power
2.	Instrument off	Turns off all instrument power
3.	Expellant valve open	Opens solenoid valve
4.	Expellant valve closed	Closes solenoid valve
5.	Cathode heater preheat	Sets the cathode heater to 4.5 A
6.	Ion gun power on	Turns on the ion gun power
7.	Ion gun power off	Turns off the ion gun power
8.	Beam voltage level 1	Sets the beam power supply to 1000 V
9.	Beam voltage level 2	Sets the beam power supply to 2500 V
10.	Keeper off	Turns the keeper supply off
11.	Discharge current level and neutralizer level 1	Sets the discharge current reference to achieve 20 mA currents; sets neutralizer emission level to 0.3 mA
12.	Discharge current level and neutralizer level 2	Sets the discharge current reference to achieve 125 mA; sets neutralizer emission level to 1 mA
13.	Discharge current level 3	Sets the discharge current reference to achieve 200 mA; sets neutralizer emission to 2 mA
14.	Neutralizer emission level 4	Sets neutralizer emission level to 2 μA
15.	Neutralizer emission level 5	Sets neutralizer emission level to 20 μA
16.	Neutralizer No. 1	Selects neutralizer filament No. 1
17.	Neutralizer No. 2	Selects neutralizer filament No. 2
18.	Neutralizer heater on	Turns on the neutralizer cathode heater
19.	Neutralizer heater off	Turns off the neutralizer heater
20.	Neutralizer bias off	Turns off the neutralizer bias power supply
21.	Neutralizer bias positive	Sets the neutralizer bias for positive polarity
22.	Neutralizer bias negative	Sets the neutralizer bias for negative polarity
23.	Neutralizer bias level 1	Turns on the neutralizer bias to 10 V
24.	Neutralizer bias level 2	Turns on the neutralizer bias to 25 V
25.	Neutralizer bias level 3	Turns on the neutralizer bias to 100 V
26.	Neutralizer bias level 4	Turns on the neutralizer bias to 500 V
27.	Neutralizer bias level 5	Turns on the neutralizer bias to 1000 V
28.	High voltage off	Turns off the beam and accel power supplies

Table 5-3. Analog Output Monitors

Channel No.	Description	Actual Value for 5 V Output, ± 5%
1	Beam current	2.5 mA (± 2%)
2	Beam voltage	2500 V
3	Discharge current	250 mA
4	Discharge voltage	50 V
5	Keeper current	250 mA
6	Keeper high voltage	1000 V
7	Keeper low voltage	50 V
8	Cathode heater current	5 A
9	Accel current*	2.5 mA
10	Decel current*	2.5 mA
11	Neutralizer heater current	5 A
12	Neutralizer bias voltage	1000 V
13	Neutralizer emission**	2.5 mA (± 10%)
14	SPIBS net current**	2.5 mA (± 10%)
15	Tank pressure	1500 psia
16	Power processor temperature	See calib curve
17	PPA AC inverter current	1.5 A
18	PPA AC inverter voltage	50 V

*To indicate anomalous condition

**In three ranges: 2.5 to 25 μA; 25 μA to 250 μA; 250 μA to 2.5 mA

5-5. ION SOURCE ASSEMBLY

The primary element of a positive ion beam system is the ion source. Its properties and requirements determine most of the specifications for other parts of the system. The ion source is characterized by the Penning discharge used to ionize the input gas. This on source type is shown schematically in Figure 5-7.
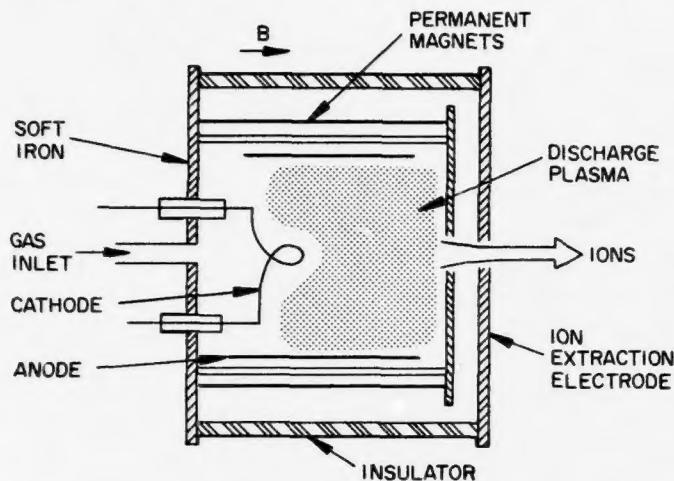
Figure 5-7. Penning
Discharge Ion Source
Schematic

5-5.1 Principle of Operation

The essential components of an ion source are the ionization chamber and the beam formation electrodes. The ionization chamber of interest here is the Penning discharge geometry shown in Figure 5-7. This discharge chamber ionizes the input gas to form a quasi-neutral plasma from which the ions are extracted and accelerated. A brief description of the ionization process is as follows. Electrons emitted from a cathode are accelerated toward the cylindrical anode. A relatively strong axial magnetic field restricts the radial electronic motion to an orbit of radius r_c, which is controlled by the magnetic field strength and the discharge voltage to satisfy the condition

$$\frac{r_a}{r_c} \geq 5 ,$$

where r_a is the anode radius. This condition having been established, electrons emitted from the cathode will be constrained in spiral orbits in the discharge diameter volume until inelastic collisions provide transport to the anode. If the gas pressure in the volume is adequate (10^{-3} to 10^{-5} Torr), a plasma will be formed, the density of which will depend on anode voltage, cathode emission, and gas pressure.

A well-focused ion beam can be formed by extracting ions through an aperture in one of the discharge chamber boundaries as shown schematically in Figure 5-8. The screen electrode is a discharge chamber boundary and the beam may be formed by using one or many sets of cylindrical apertures like the ones shown in Figure 5-8.

55
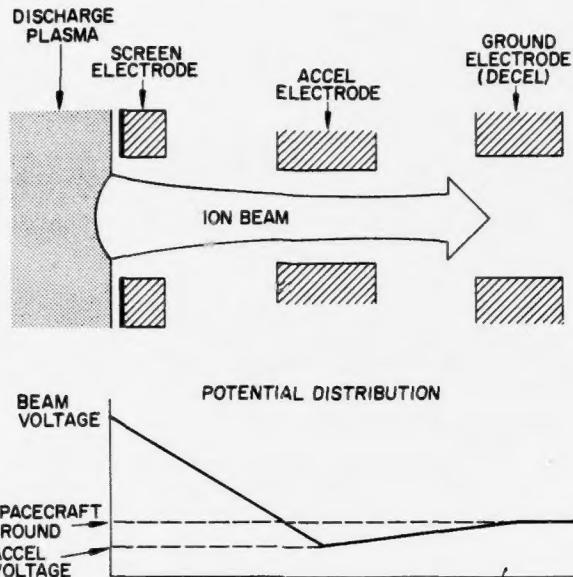
Figure 5-8. Ion Beam Focusing Schematic Diagram

The beam is extracted and focused by applying appropriate voltages to the elec-
trodes as shown in the potential distribution diagram of the figure. By appropriate-
ly adjusting the discharge plasma density, a given electrode design will form a
well-focused beam with current I related to the total extraction voltage V by the
expression

$$I = PV^{3/2},$$

where P is the effective perveance. The total voltage is the numerical sum of the
beam and acceleration voltages. The perveance defined above depends on the ion
mass and it is common practice to speak of the electrode design in terms of
electron perveance P_e, where P_e is related to P by the square root of the mass ratio

$$\frac{P}{P_e} = \sqrt{\frac{m_e}{m}},$$

where m and m_e are the ion and electron mass ratios, respectively. Typical
extraction electrode designs, which have been used with the source under considera-
tion here, have perveances P_e, varying from 0.1 to 2 μperv.

56